



Exploring the Inelastic Dark Matter frontier with the CRESST experiment

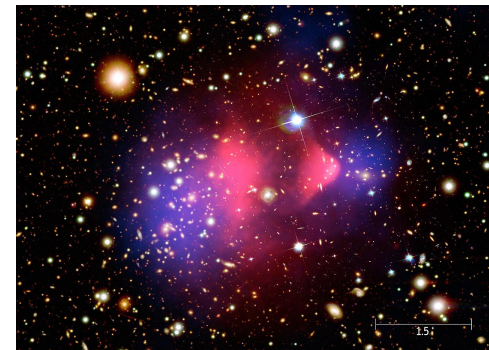
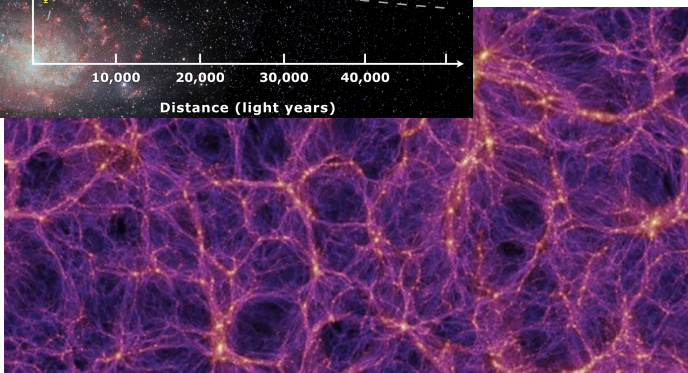
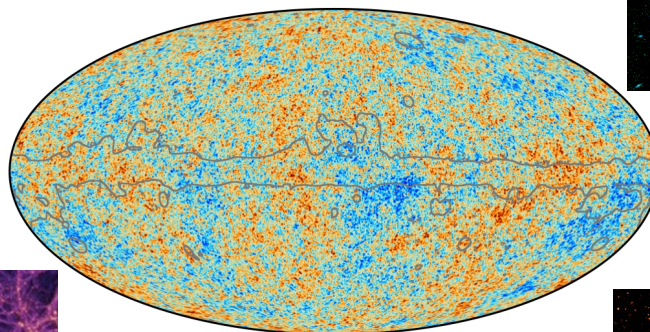
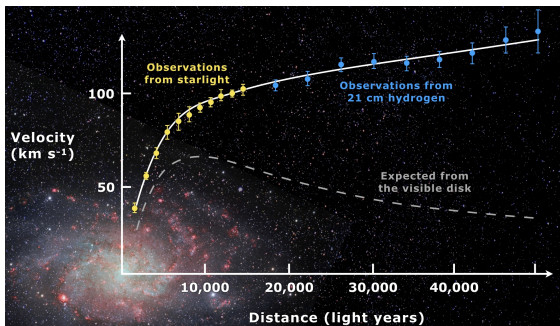
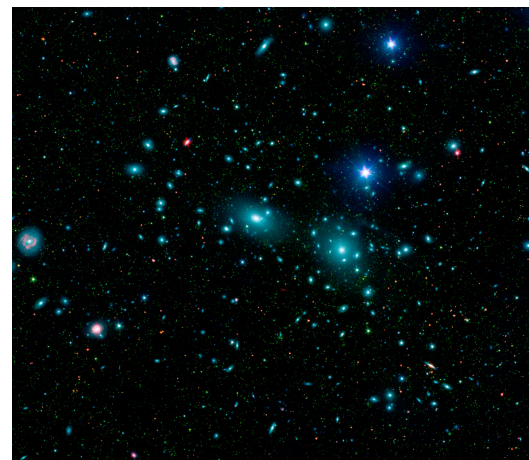
Miriam Olmi



The quest for Dark Matter

Evidence for Dark Matter

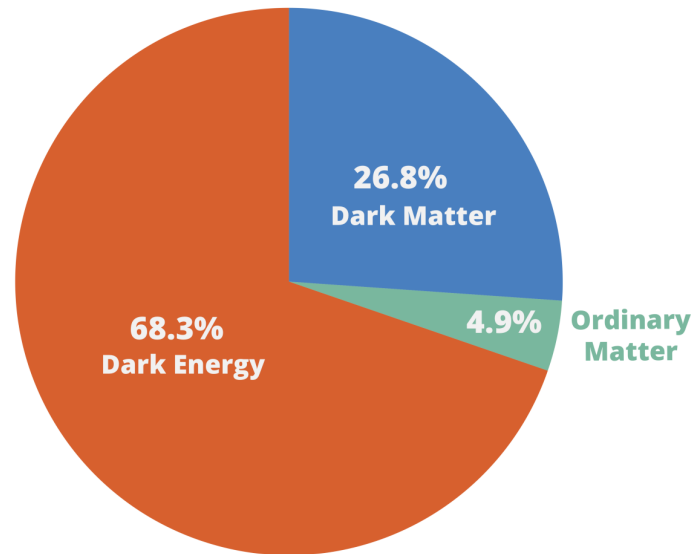
- Velocity dispersion & Coma cluster
- Galactic rotation curve
- Gravitational lensing and Bullet Cluster
- Cosmic Microwave Background
- Structure formation
- And others..



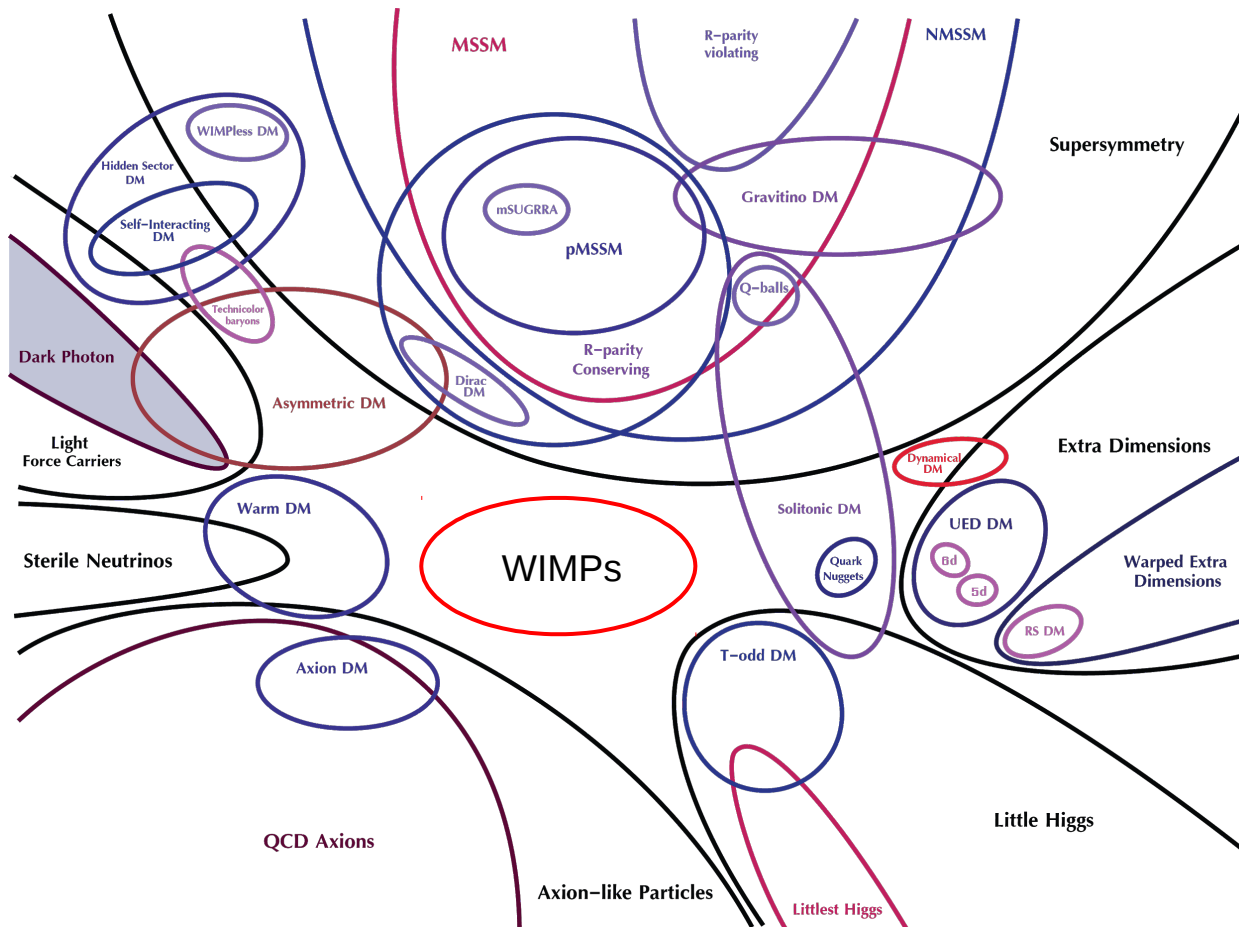
Evidence for Dark Matter

Known information:

1. stable (long life-time)
2. interacting gravitationally
3. non interacting em
4. cold, i.e. not relativistic
5. average energy density
6. nearby energy density



Models and candidates



From T. Tait

Detection of DM particles

- Colliders
- Indirect search
- Direct search

Basic assumption: DM particles are naturally produced during interaction of particles beams
NB: collider searches cannot prove dark matter

Basic assumption: Annihilation or decay products of DM particles result in detectable species, especially gamma rays, neutrinos and antimatter particles

Basic assumption: DM particles interact weakly via elastic and inelastic scattering with atomic nuclei or with electrons in the detector material

Standard DM halo

Existence of a halo surrounding galaxies confirmed by galaxy rotation curve observations

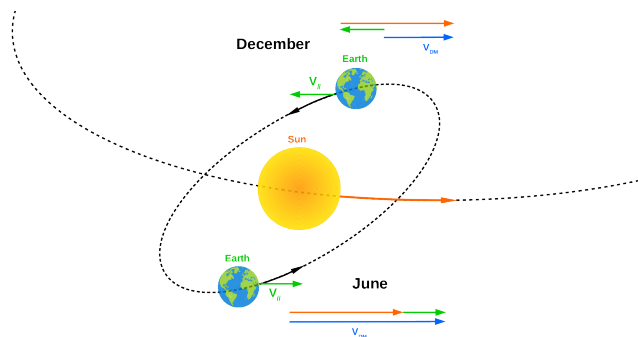
⇒ Halo model = key point for DM searches

Standard halo model

Spherical halo with Maxwell-Boltzmann velocity distribution truncated at the escape velocity of the galaxy ~ 533 km/s

Local DM density: ~ 0.3 GeV/cm³

Dark Matter halo



Annual modulation

Elastic Dark Matter rate

Scattering targets per unit mass

$$\frac{dR}{dE_R dM} = n_\chi N_T \int_{v > v_{min}} v f(\vec{v}, \vec{v}_e) \frac{d\sigma}{dE_R} d^3v$$

Astrophysical input

$$n_\chi = \frac{\rho_\chi}{m_\chi}$$

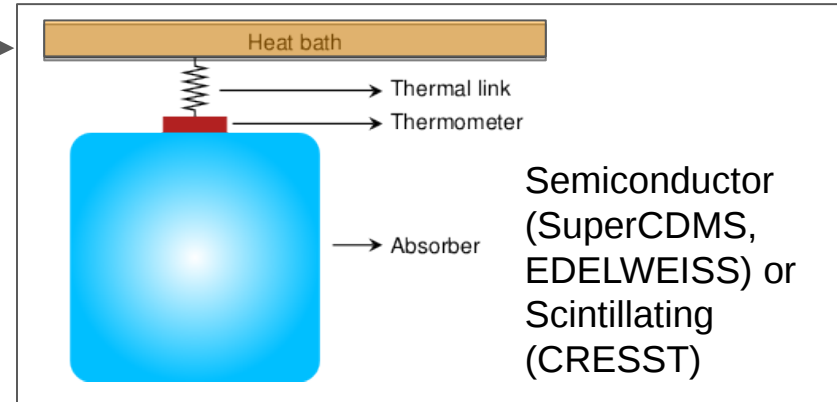
Nuclear physics input

$$\frac{d\sigma}{dE_R} = \frac{\sigma_n m_N [Z f_p + (A - Z) f_n]^2}{v^2 2\mu_n^2 f_n^2} F^2(E_R)$$
$$v_{min} = \sqrt{\frac{E_R m_N}{2\mu^2}}$$

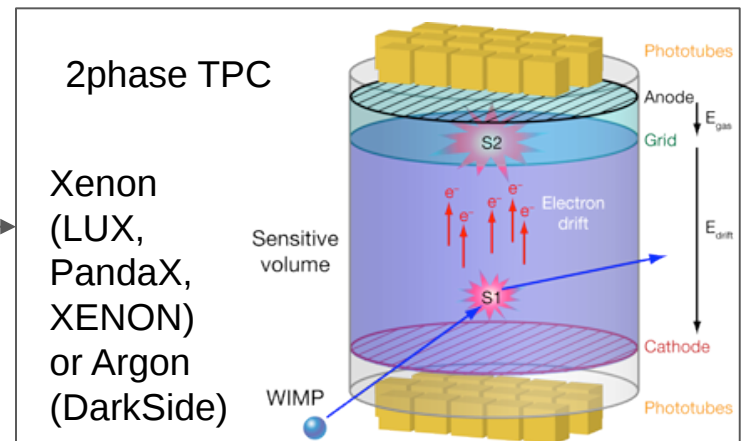
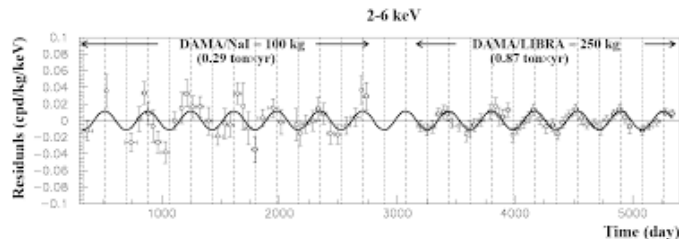
Experimental approaches for direct detection

Incoming particle with $v/c \sim 10^{-3} \Rightarrow$ DM mass in [1-100] GeV \Leftrightarrow NR energy from 100 to 0.1 keV

- Solid-state cryogenic detectors
- Noble liquids detectors
- Room temperature scintillating detectors
- Room temperature ionisation detectors
- Super-heated liquid detectors
- Directional detectors

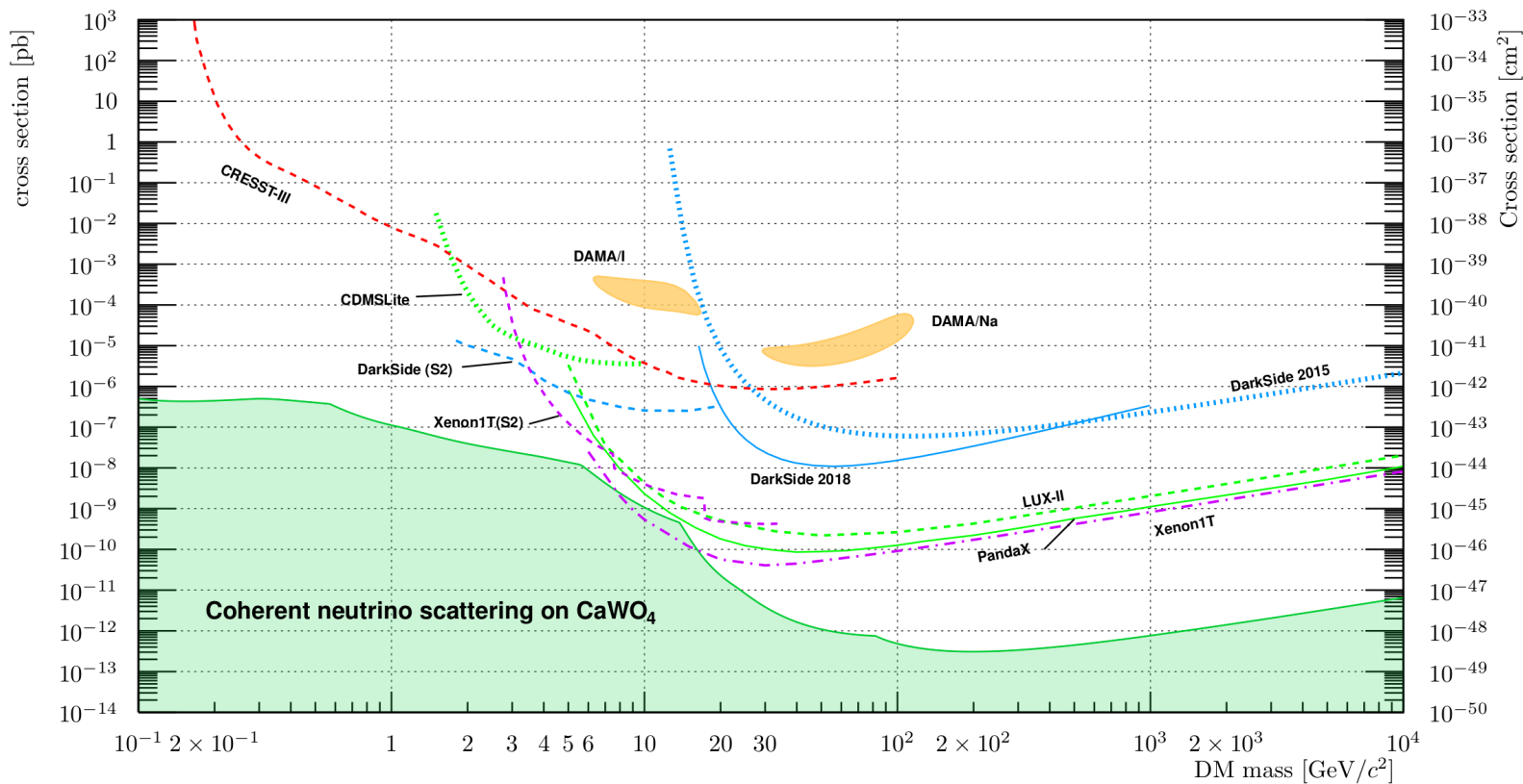


High-purity NaI crystals (DAMA, ANAIS, COSINE-100, SABRE, COSINUS)
DAMA/LIBRA annual modulation at 12.9σ C.L.

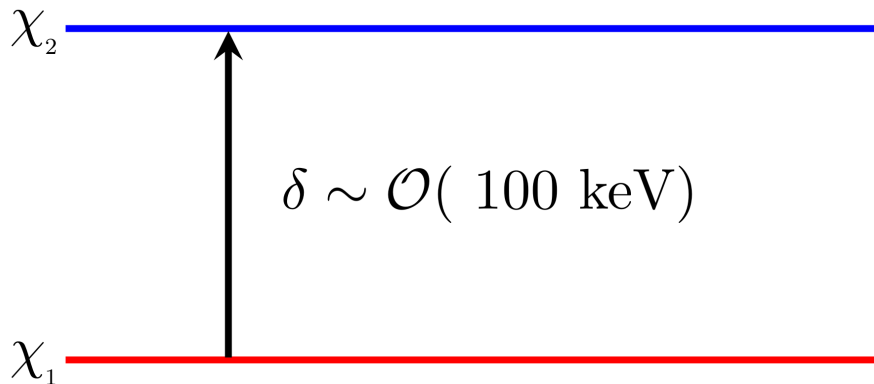


State of the art

Standard scenario: WIMPS+elastic scattering+standard halo



Inelastic Dark Matter framework



Dark Matter scatters off nuclei into an excited state with mass splitting broadly in the hundreds of keV range

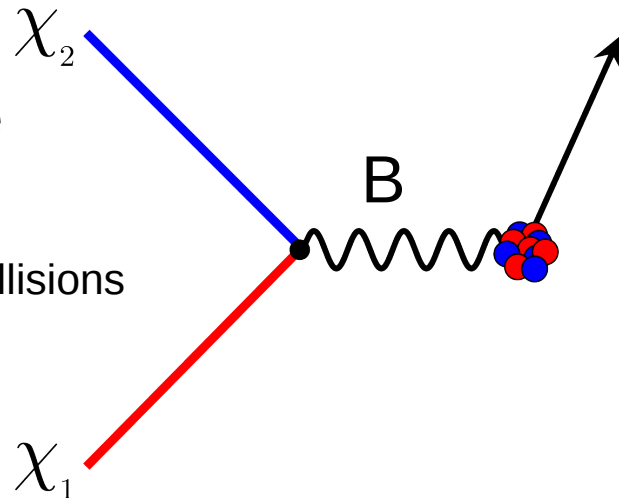
In the final state after the interaction the mass of the outgoing particle is different with respect to the one of the incoming particle

Inelastic Dark Matter framework

Fundamental assumption: The inelastic interaction is obtained via a vertex of the type $\chi_1\chi_2 B$ where χ_1 is the primary DM agent, χ_2 is the DM excited state and B is a new mediator so that the elastic scattering is not possible.

Basic consequences:

- The initial kinetic energy of [χ_1 +nuclear sys.] must be greater than δ for the scattering to take place
- Minimum required energy for inelastic DM-nuclear collisions implies a minimum recoil energy in the detector
- Available kinematic phase space is reduced and the rate is suppressed



Inelastic Dark Matter framework

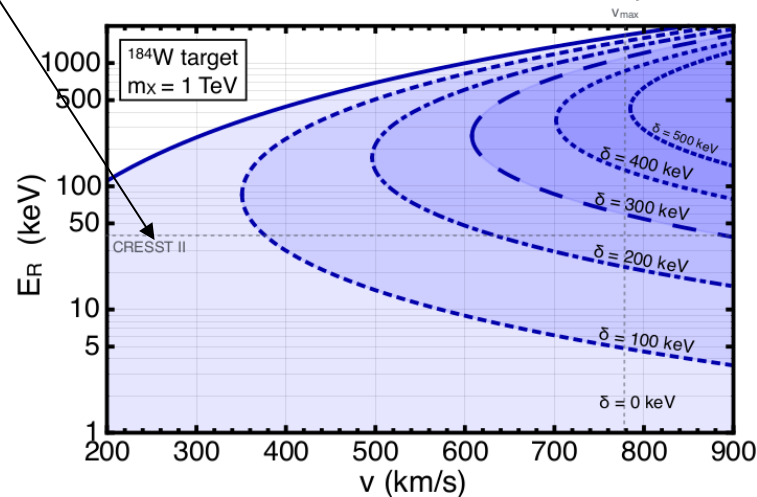
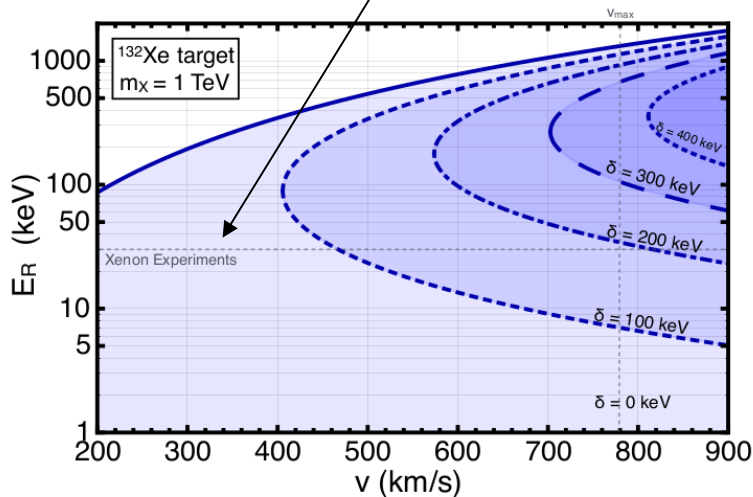
- Inelastic DM proposed more than 20 years ago
- iDM remain a very interesting hypothesis to be probed as its spectrum is completely different with respect to the standard one
- Bramante et al. studied the iDM expected signal for several experiments with different target material and CRESST resulted to be the most suitable to explore the iDM scenario with high mass splittings (>350 keV) thanks to the presence of Tungsten in its target

→ [J. Bramante, P. J. Fox, G. D. Kribs and A. Martin, Inelastic frontier: Discovering dark matter at high recoil energy, Phys. Rev. D94 \(2016\) 115026, \[1608.02662\].](#)

Inelastic Dark Matter framework

Expected *maximum* incoming terrestrial dark matter speed ~ 780 km/s

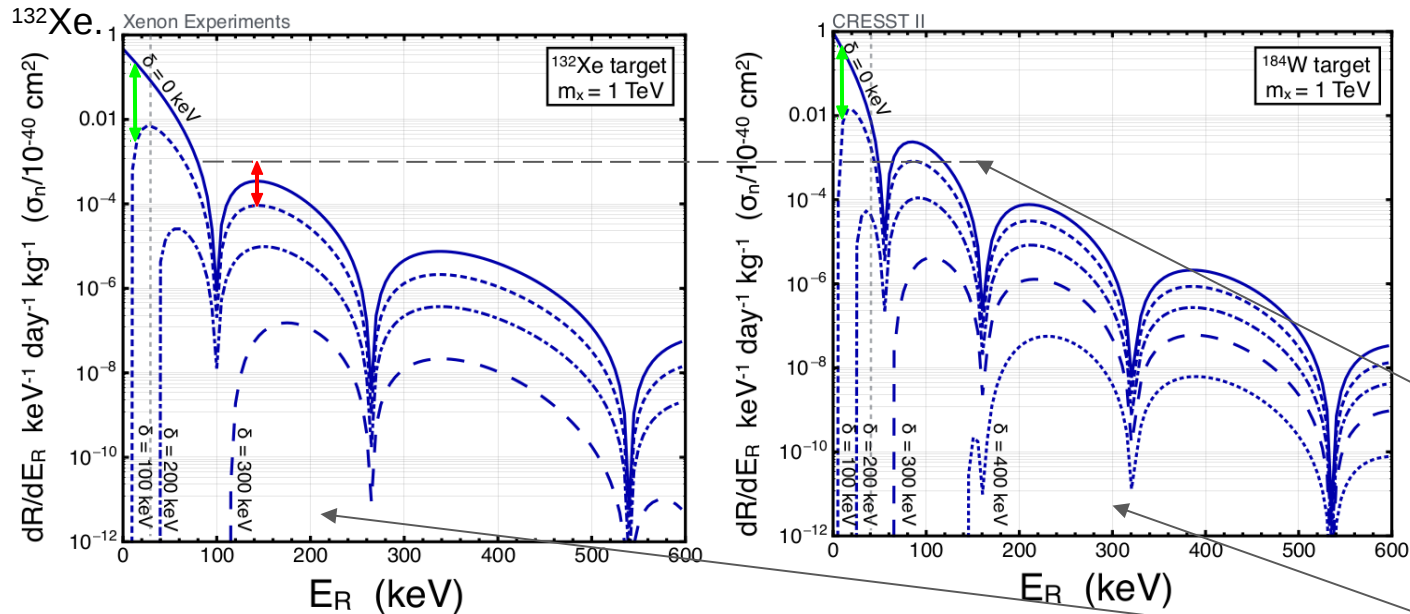
Maximum recoil energy windows used by the relative experiments



The shaded region is the available range of recoil energies on a nuclear target for a given DM mass splitting and incoming DM speed in the laboratory frame
 \Rightarrow CRESST experiment has access to higher mass splittings

Inelastic Dark Matter framework

Expected rate for dark matter nucleon scattering per kg per day and per keV of nuclear recoil energy, assuming a DM-nucleon cross-section $\sigma_n = 10^{-40} \text{ cm}^2$, a DM mass of 1 TeV and a target made purely of ^{184}W or ^{132}Xe .



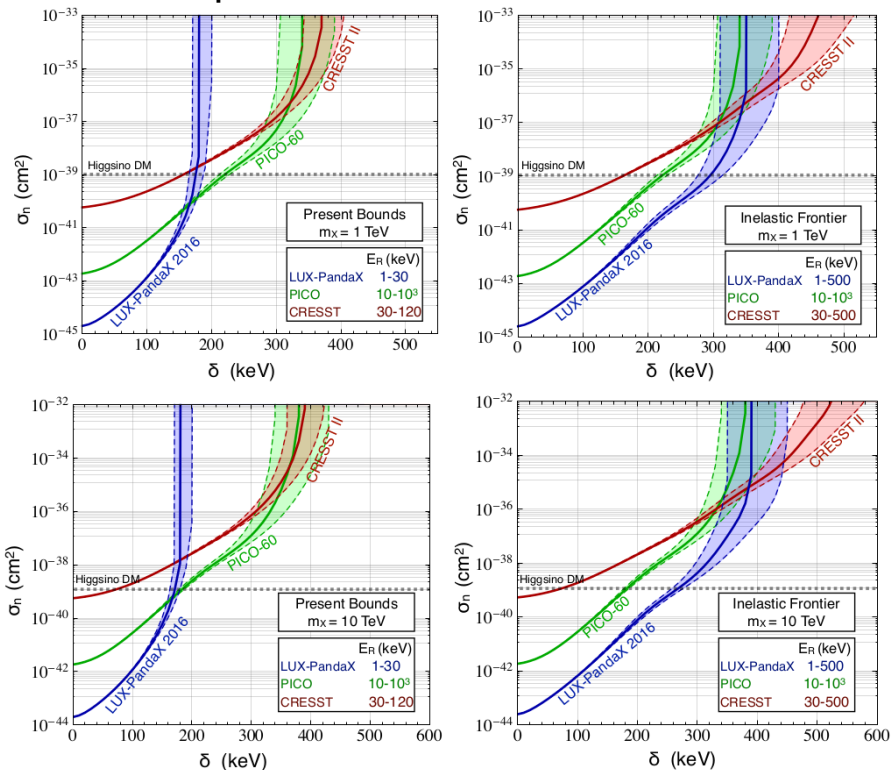
Suppressed rate of iDM

Heavier target material
 ➤ Higher rate
 ➤ Larger mass splitting available

$$\frac{dR}{dE_R dM} = n_X N_T \int_{v_{min}}^{v_{max}} v f(\vec{v}, \vec{v}_e) \frac{d\sigma}{dE_R} d^3v.$$

Inelastic Dark Matter framework

Exclusion plots for dark matter nucleon scattering

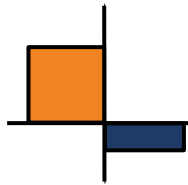


Present energy regions compared with inelastic DM hp, i.e. higher recoil energies included in the analysis

Experiment	Exp. (t-days)	Refs.
PICO	1.3	Phys. Rev. D93 (2016) 052014
LUX	14	Phys. Rev. Lett. 116 (2016) 161301
PandaX	33	Phys. Rev. Lett. 117 (2016) 121303
CRESST	0.052	Eur. Phys. J. C76 (2016) 25

Limits obtained with data from the table and assuming integrated luminosities, event rates, and nuclear masses.

J. Bramante, P. J. Fox, G. D. Kribs and A. Martin, [Inelastic frontier: Discovering dark matter at high recoil energy](#), [Phys. Rev. D94 \(2016\) 115026](#), [[1608.02662](#)].



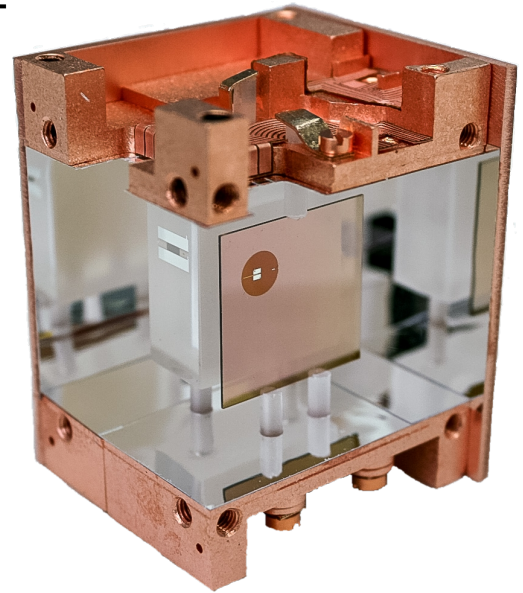
The CRESST experiment

The CRESST experiment

- CRESST is a cryogenic experiment for direct detection of DM.
- Detector target = CaWO_4 crystals
- Characterized by:
 - Low energy threshold
 - Good energy resolution
 - Particle identification thanks to 2 channel readout

Now optimized for low mass DM detection.

My work focused on another key feature of the CRESST experiment: its target. Thanks to Tungsten CRESST is the experiment with the heaviest target element currently employed in dark matter searches.



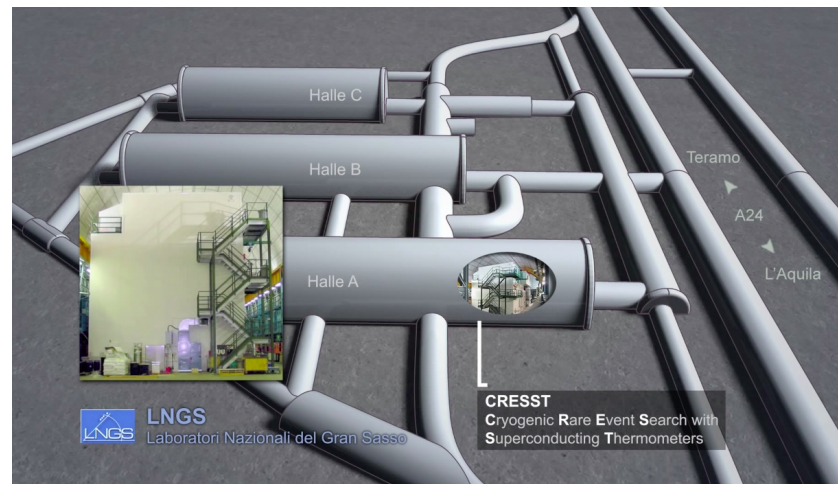
CRESST is the most suited experiment to probe the iDM frontier.

The CRESST experiment

Cryogenic Rare Event Search with Superconducting Thermometers

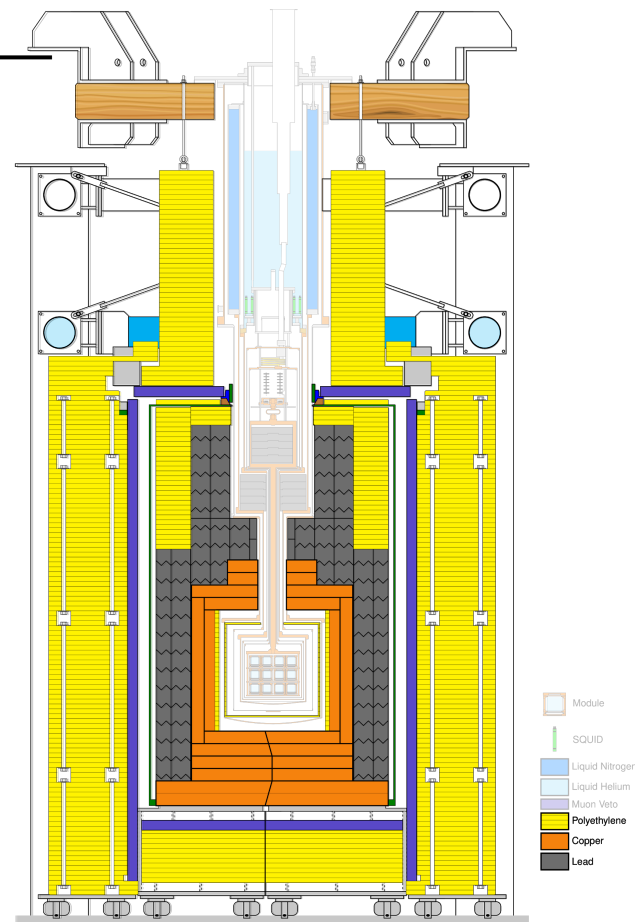
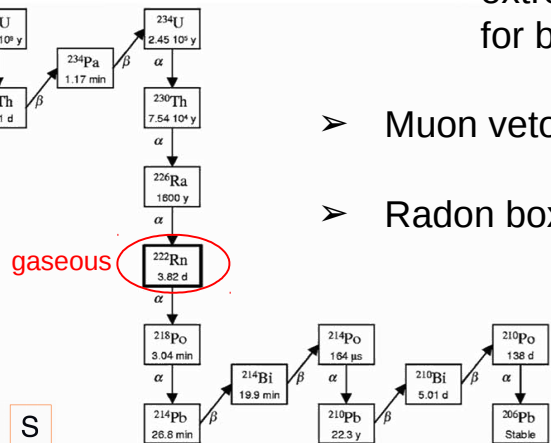
CRESST is a direct DM search experiment located at Laboratori Nazionali del Gran Sasso (LNGS, Italy)

- Rock overburden $\sim 1400\text{m}$ in all directions (3800 m.w.e.)
- Muon flux reduced of a factor 10^{-6}

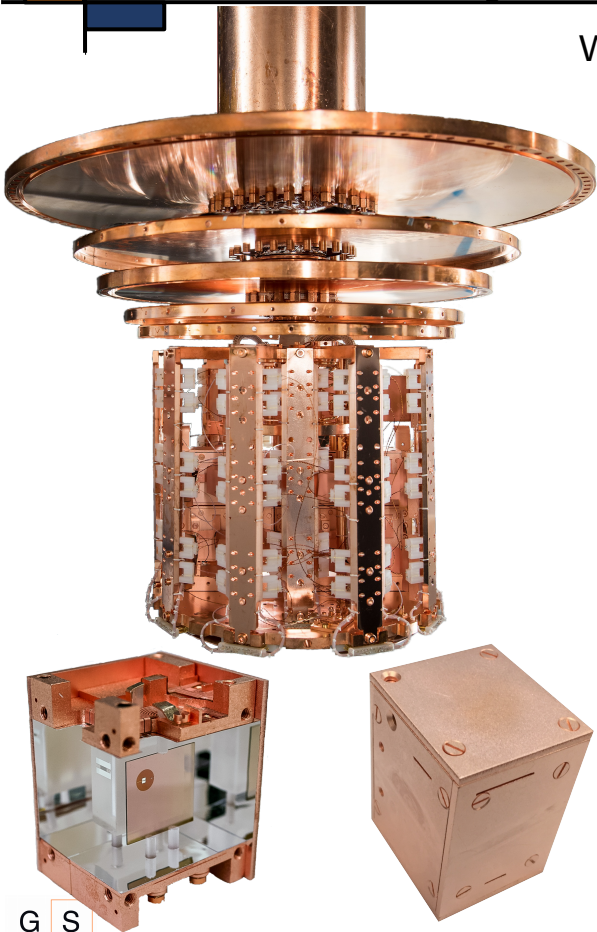


Background and shielding

- Polyethylene shield (2 layer) for neutrons' thermalisation
- Lead shield for beta/gamma(alpha) radiation
 ^{210}Pb isotope not stable
 production of radiation until ^{206}Pb is reached
- Copper shield extremely clean material for betas and gammas from lead shield
- Muon veto
- Radon box

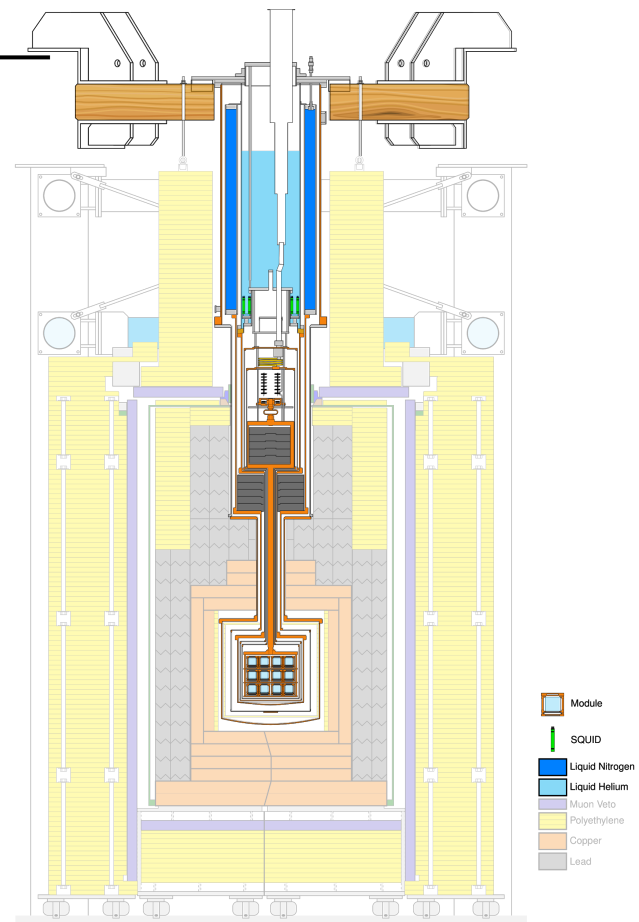


CRESST cryostat

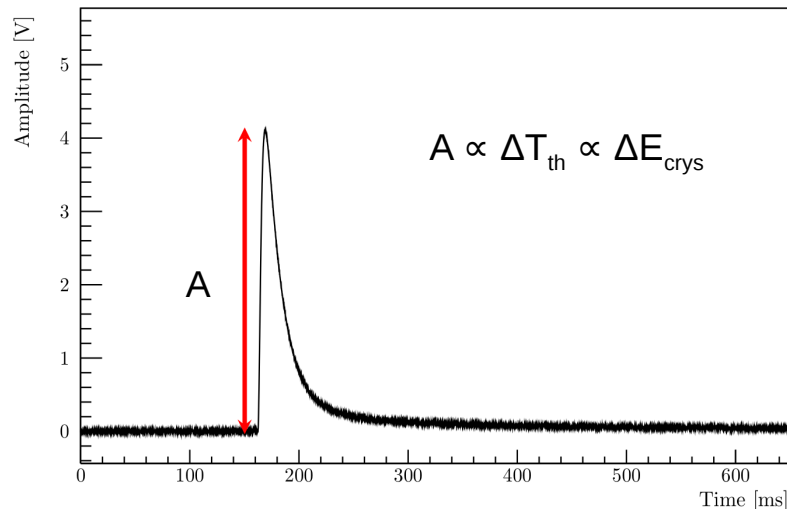
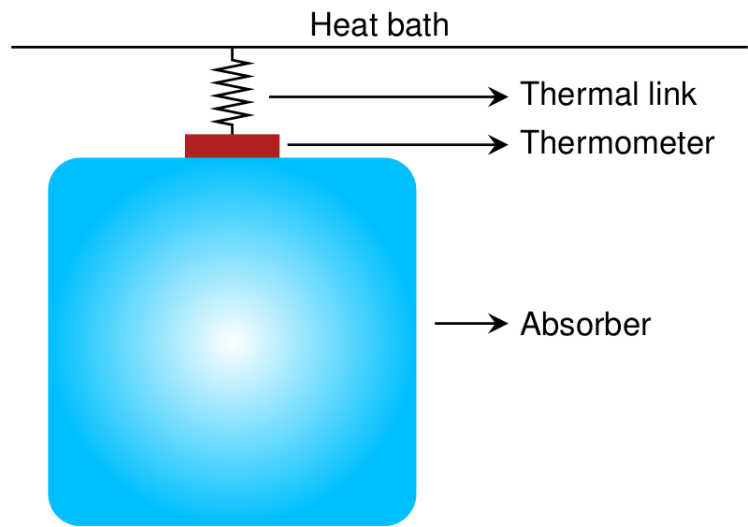


Working temperature $\sim 10\text{mK}$

- Dilution refrigerator based on the mixture of ^3He and ^4He
- LNitrogen vapor and LHelium tanks
- Additional lead to shield the detector from the dilution refrigerator
- Air dampers to attenuate external vibrations
- 5 thermal shield at decreasing temperatures
- “Cold finger”: copper rod 1.5 m long
- Carousel with detector modules



Cryogenic detector



Heat capacity above transition of the thermometer:

$$C_{th} = A T + B T^3$$

Electronic contribution

Lattice contribution

$$\Delta T_{th} = \frac{\Delta E_{th}}{C_{th}} \propto \frac{\epsilon \Delta E_{crys}}{C_{th}}$$

Collection efficiency of phonons produced in the crystal

CRESST detector: working principle

Phonon Detector (PD)

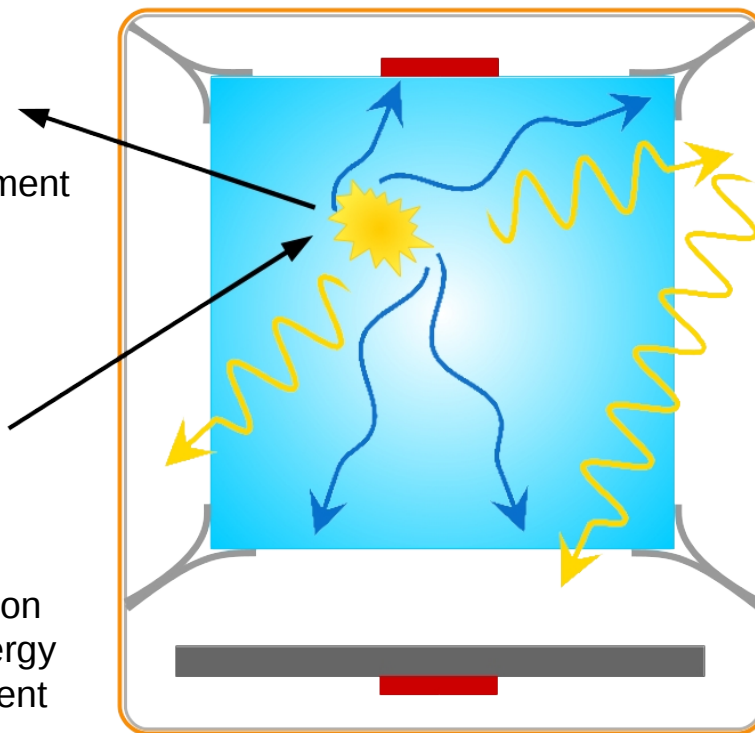
⇒ precise energy measurement

- $\geq 90\%$ total energy
- Particle independent

Light Detector (LD)

⇒ particle discrimination

- Few % total energy
- Particle dependent



Reflective and scintillating foil

- To improve scintillation light collection efficiency
- Additional active veto

active housing



Rejection of events due to an eventual superficial contamination

CRESST detector

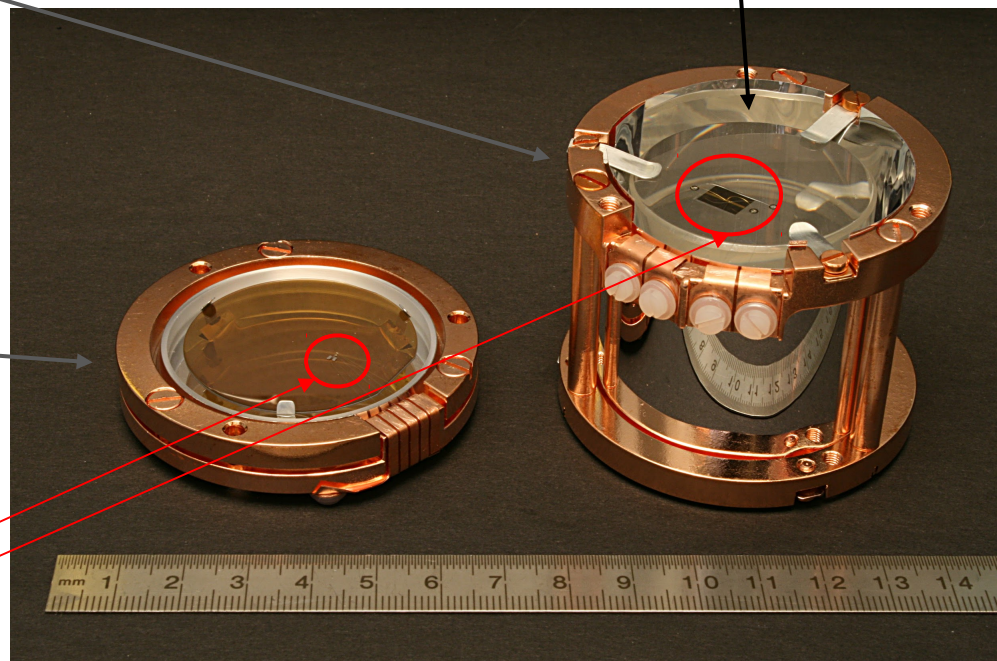
Phonon Detector (PD)
Cryogenic calorimeter
M ~ 300 gr of CaWO_4

Scintillating
crystal

Light Detector (LD)
Sapphire wafer coated with
thin layer of Silicon

Both equipped with
special thermometers

Reflecting and scintillating foil

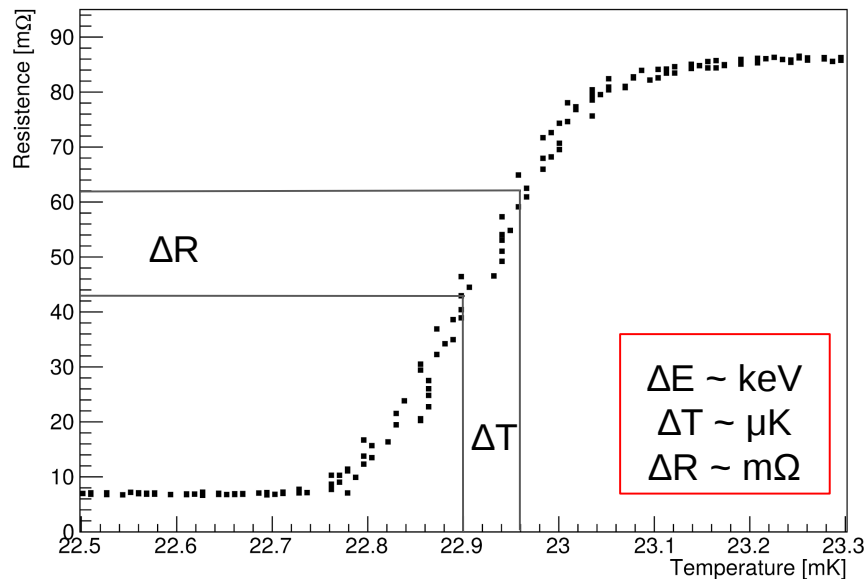


Transition Edge Sensor

Thin layer of Tungsten working in its transition between the super- and the normal-conducting phase.

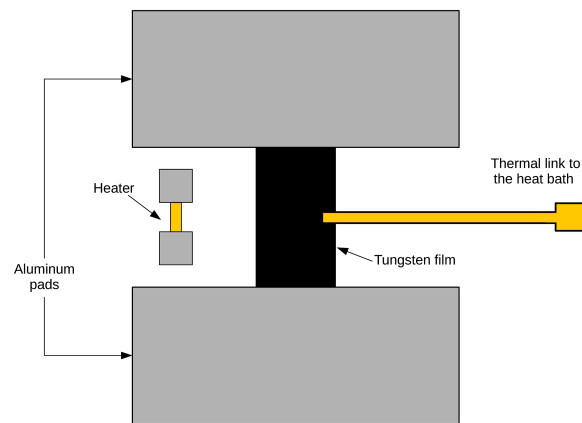
$$T_c^W \sim 15 \text{ mK}$$

$$T_c^{TES} \simeq [15; 30] \text{ mK}$$

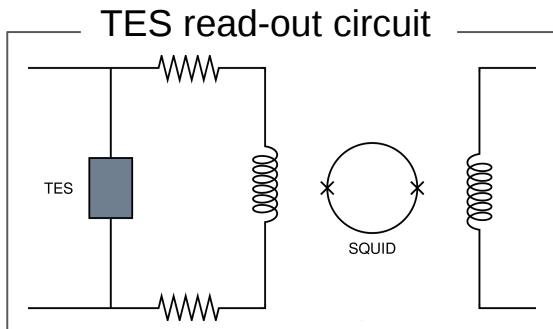


Additional structures:

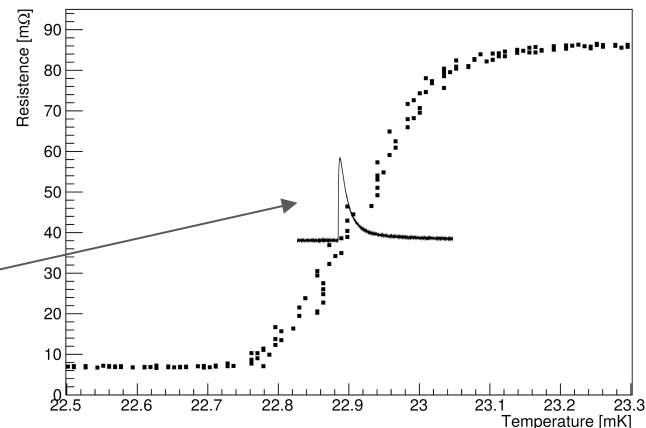
- Aluminum pads to maximize collection efficiency
- Heater to set the working point of each sensor



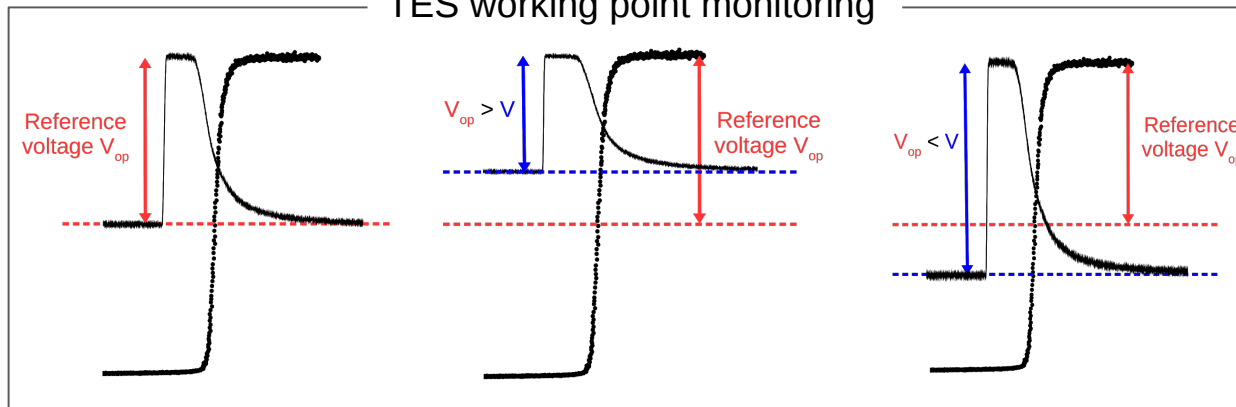
Transition Edge Sensor



Short linear range

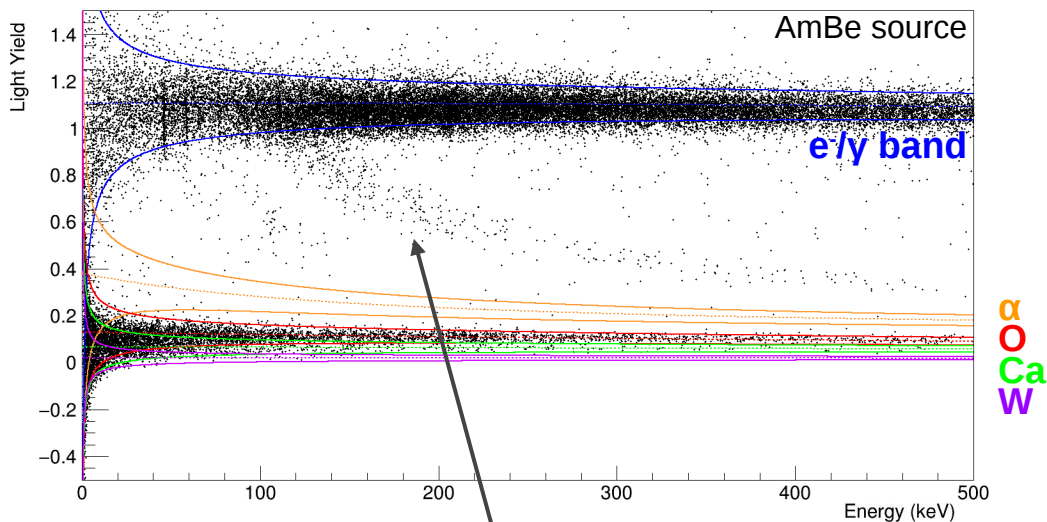


TES working point monitoring



Particle identification & Background discrimination

$$\text{Light Yield} = \frac{\text{Energy in the LD}}{\text{Energy in the PD}}$$



Inelastic scattering of neutrons off Tungsten nuclei

$$QF^X(E_{\text{dep}}) = \frac{\text{Light produced by X when depositing } E_{\text{dep}}}{\text{Light produced by } \gamma \text{ when depositing } E_{\text{dep}}}$$

- Precise values of QFs obtained with dedicated measurements
- Observed variations $\sim O(10\%)$ between different crystals

iDM search with CRESST

- Thanks to Tungsten CRESST can probe larger mass splittings
- Due to the suppressed rate of the iDM a larger exposure is preferable

CRESST-II

2013-2015

$M_{\text{crys}} \sim 300 \text{ gr}$

CRESST-III

2016-today

$M_{\text{crys}} \sim 24 \text{ gr}$

CRESST-II more suited to explore the iDM frontiers due to the larger mass

- Higher exposure
- Wider linear range

CRESST-II detectors overview

Standard design

VK31 (307 gr) VK34 (304 gr)
VK32 (308 gr) Verena (306 gr)
VK33 (310 gr) Daisy (307 gr)

Small TES carrier

Anja (308 gr) Zora (302 gr)
Lise (306 gr) Wibke (308 gr)
Frederika (266 gr)

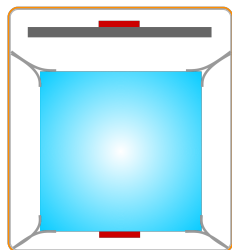
Sticks design TUM40 (248 gr)

Beaker design

VK28 (194 gr)
VK27 (197 gr)

Carrier design

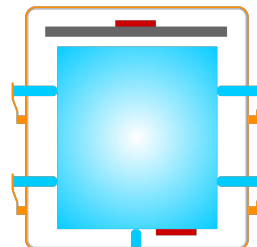
TUM38 (299 gr)
TUM29 (299 gr)



Std. design



Carrier design



Stick design

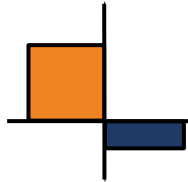


Beaker design

- Different detector designs
- Different crystal radiopurity
- Different TES performances (working point and linear region)

⇒

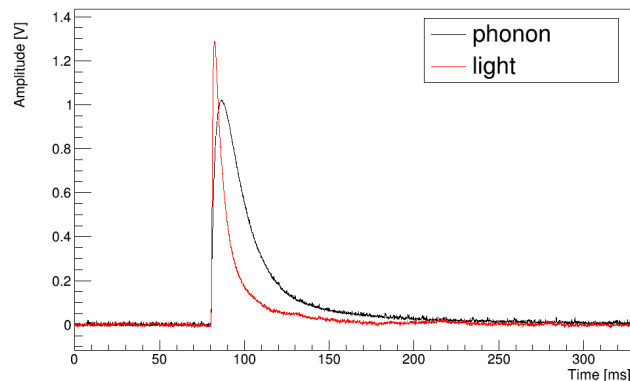
very different detector responses to study and analyse individually to find the detector modules with the best performances for the iDM search



Raw data analysis

Event types

An event in CRESST consists of 2 coincident signals: Phonon + Light
Both channels are always acquired regardless of which one triggered



- Control pulses: large heater pulses needed to monitor the TES working point
- Test Pulses (TP): heater pulses with small and varying amplitudes to export the calibration in the whole data set
- Empty baselines: acquired with artificial trigger and needed for a precise measurement of the noise
- Particle pulses: real trigger events due to particle interactions in the detector

Data sets



Energy calibration with the 122 keV γ -line
Both channels expressed in keV_{ee}

Long physics run whose data are used for the iDM analysis (data quality cuts & high level analysis)

γ calibration with ^{57}Co data

Background dataset

Neutron calibration data

Study of the response of every individual detector module to neutron-induced nuclear recoils for a precise determination of QFs as they can vary between different crystals $\sim O(10\%)$

Analysis chain

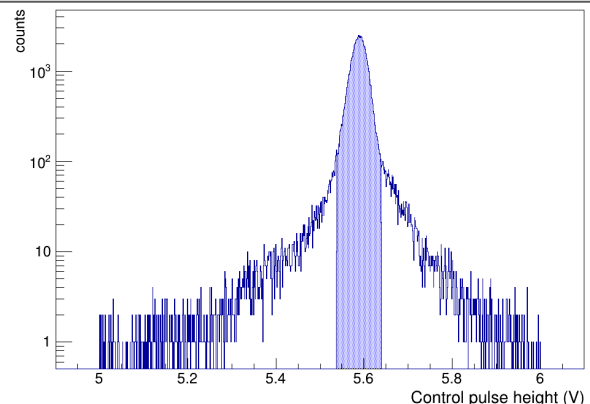
- 1) Raw parameters evaluation
- 2) Truncated fit procedure
- 3) Correction of time-dependent effects
- 4) Energy conversion

→ common to all the data of the three data sets

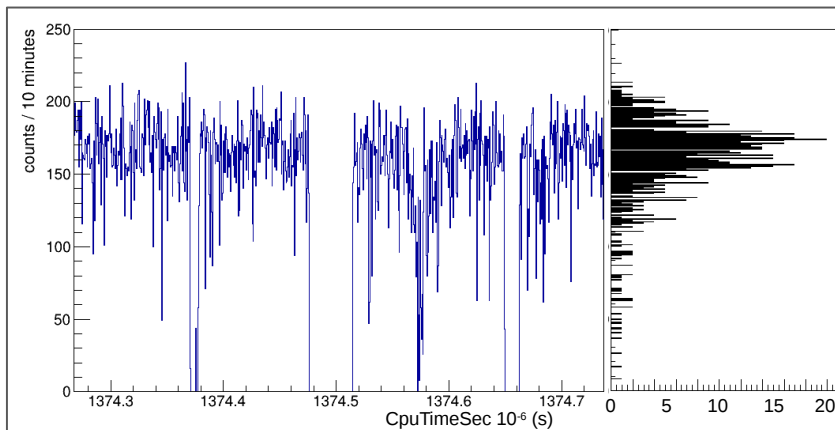
Stability and Rate Cut

Stability Cut

To remove events in which the TES is out of its correct working point.
Done with Control pulses distribution.



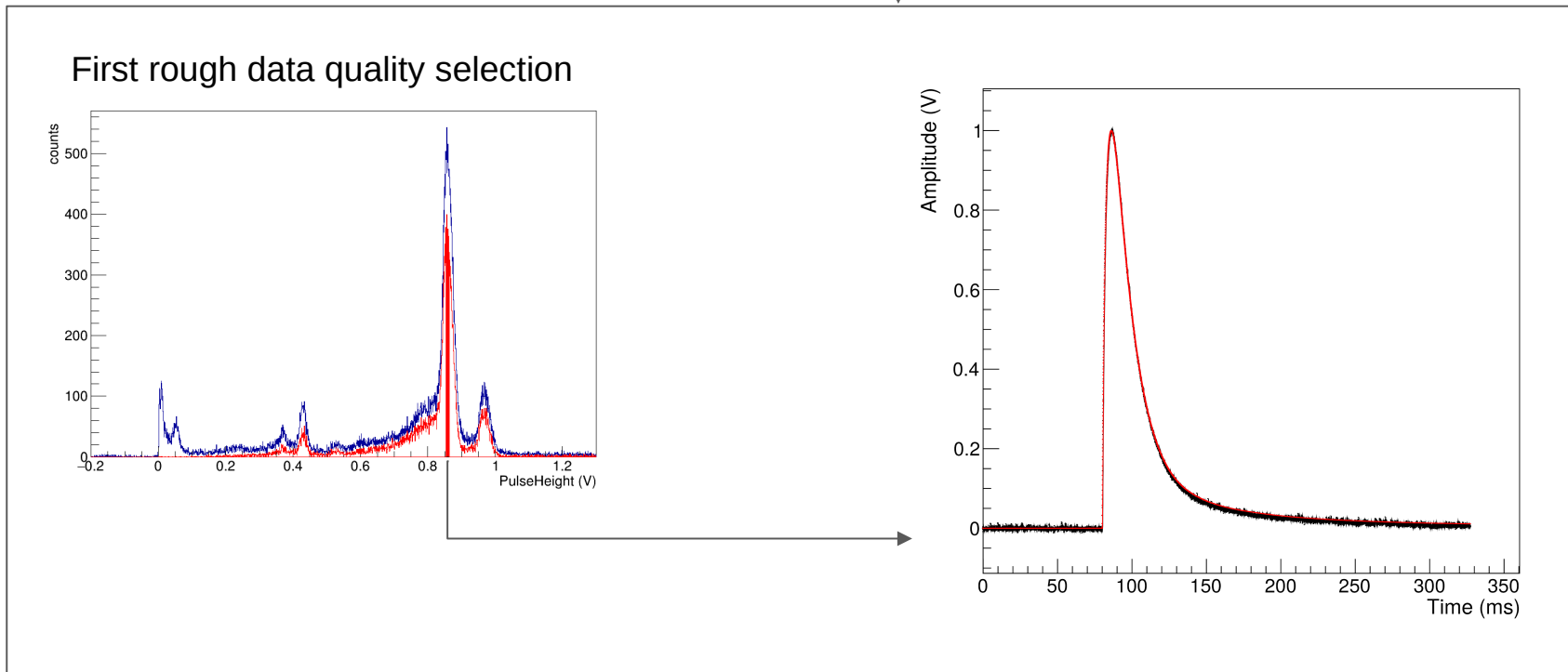
Rate Cut



To remove high trigger rate periods (electronics and environmental disturbances, microphonics..)

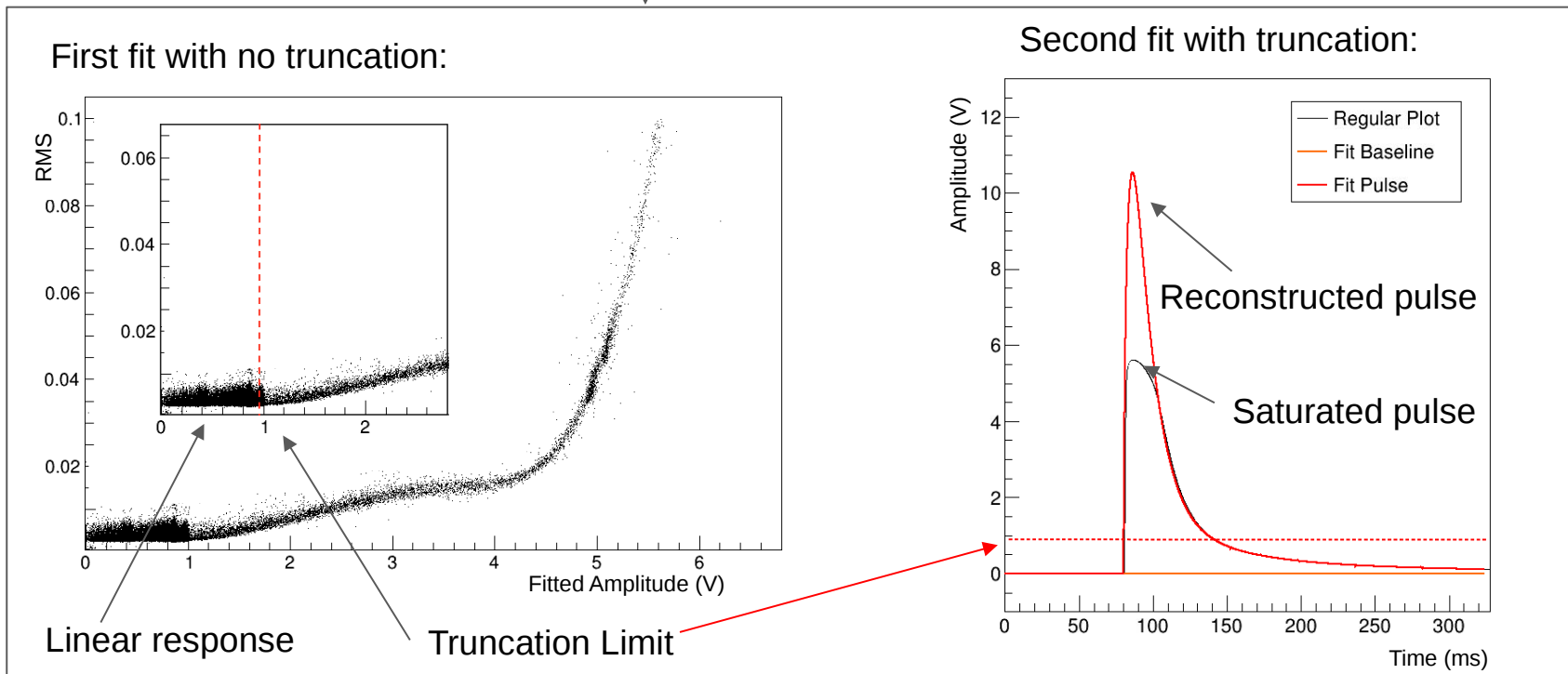
Gamma calibration data

1. Raw parameter estimation
 - a. Template creation (average pulse)



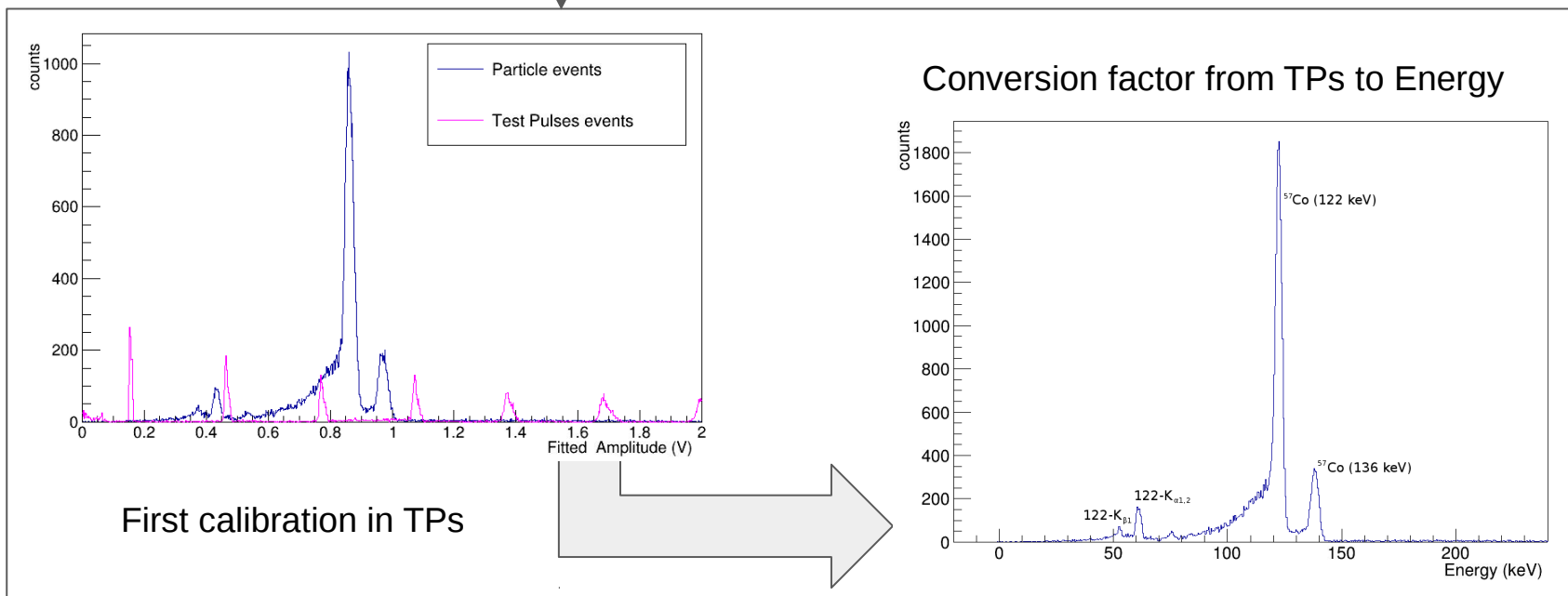
Gamma calibration data

1. Raw parameter estimation
2. Truncated fit procedure



Gamma calibration data

1. Raw parameter estimation
2. Truncated fit procedure
3. Correction of time-dependent effects
4. Energy conversion

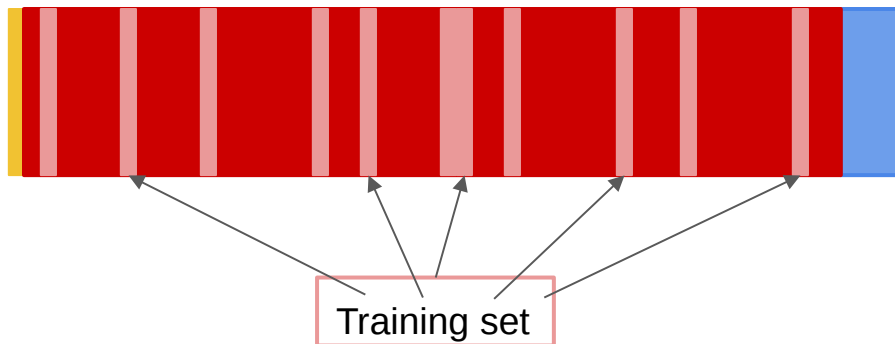


Background data

Total exposure ~ 160 kg day for each detector module

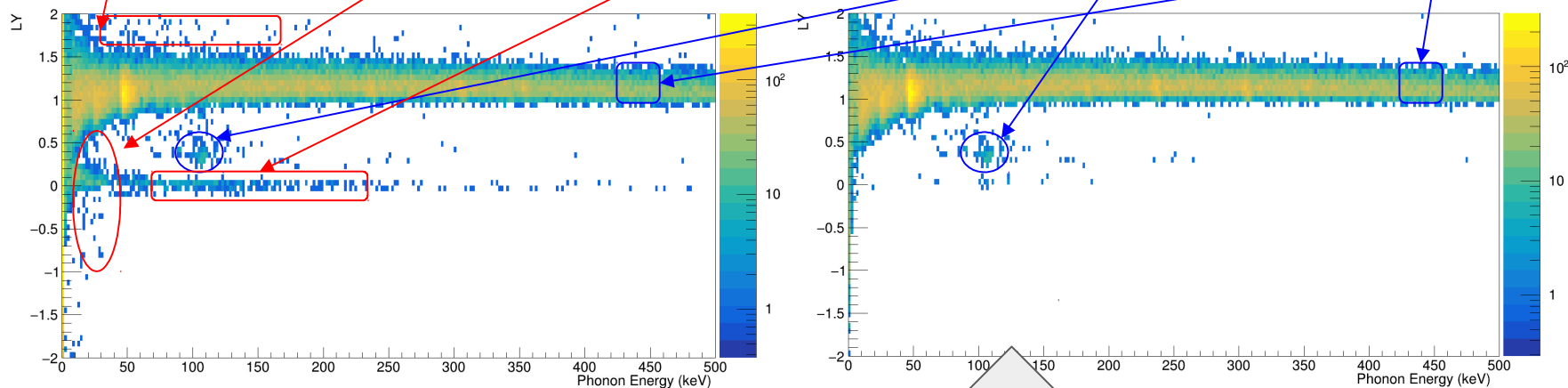
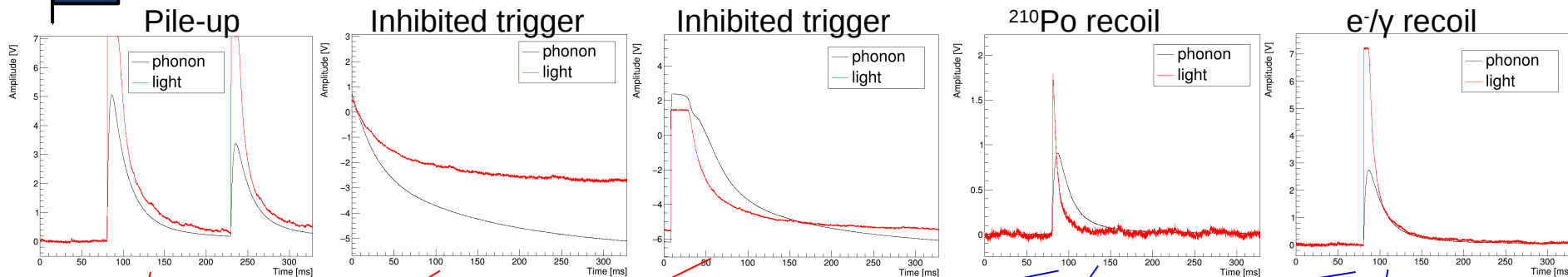
To avoid any unwanted bias a **blind analysis** is performed.

- I. All the selections are developed using only 20% of the full dataset randomly selected (training set)
- II. Then they are applied, with no modification, to the full data set

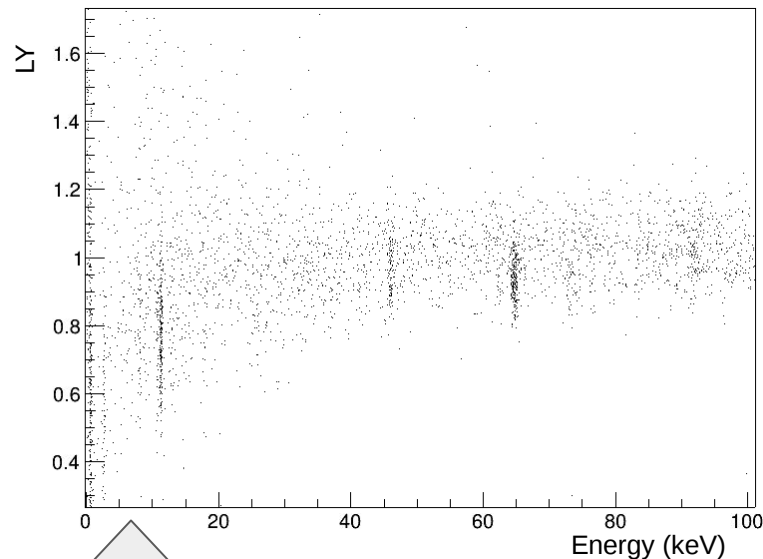
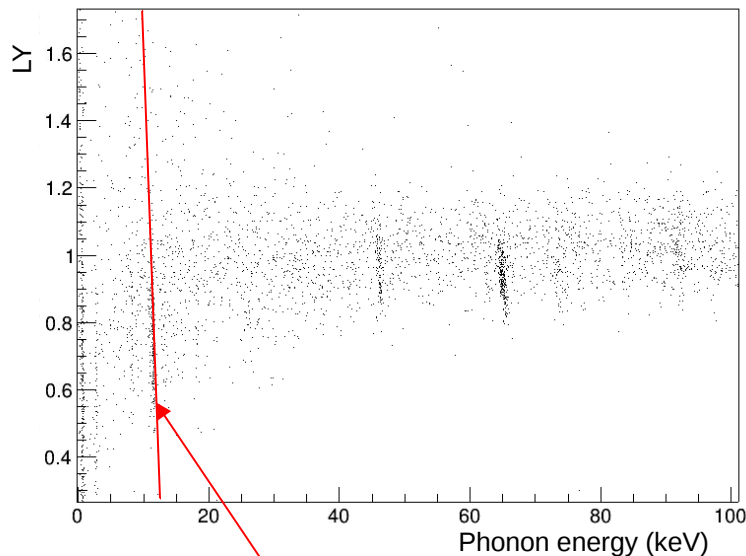


Background data

Module Verena



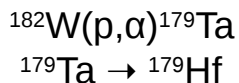
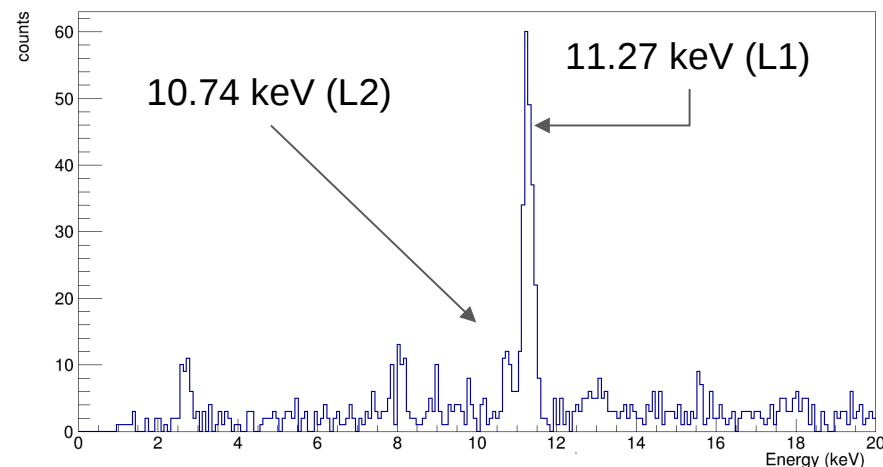
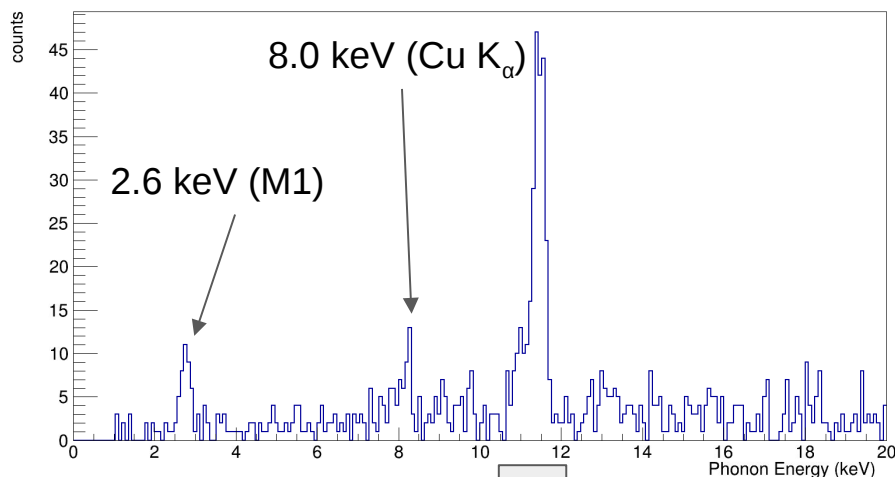
1. Energy shared between PD and LD \rightarrow 2 channels anticorrelated \rightarrow γ -lines in LY:E plot tilted
2. Precise energy reconstruction = energy in PD + energy in LD
3. Correcting the γ -lines tilt improve the energy resolution



11 keV γ line fitted with:
 $LY = 1 - (E_p - E_\gamma) / \eta$

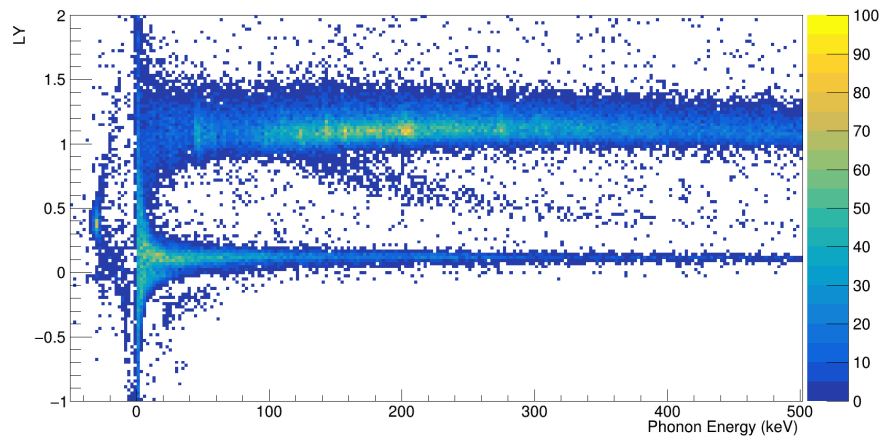
$$E = [1 - \eta (1 - LY)] E_p$$

1. Energy shared between PD and LD \rightarrow 2 channels anticorrelated \rightarrow γ -lines in LY:E plot tilted
2. Precise energy reconstruction = energy in PD + energy in LD
3. Correcting the γ -lines tilt improve the energy resolution

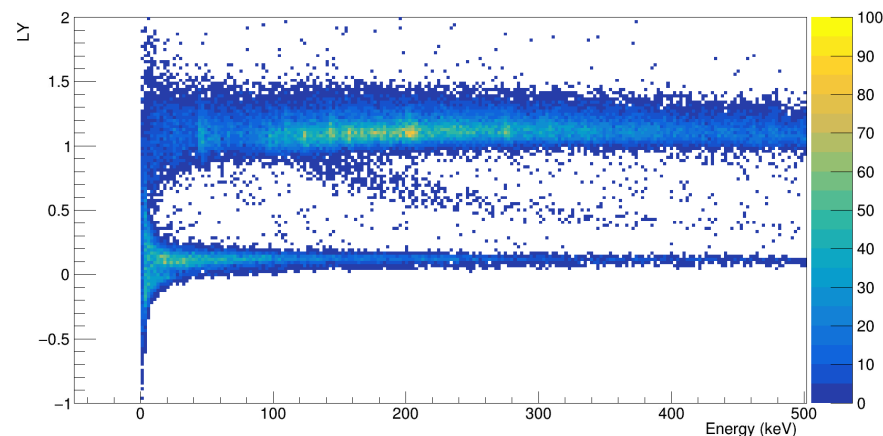


$$E = [1 - \eta(1 - LY)] E_p$$

Before data quality cuts

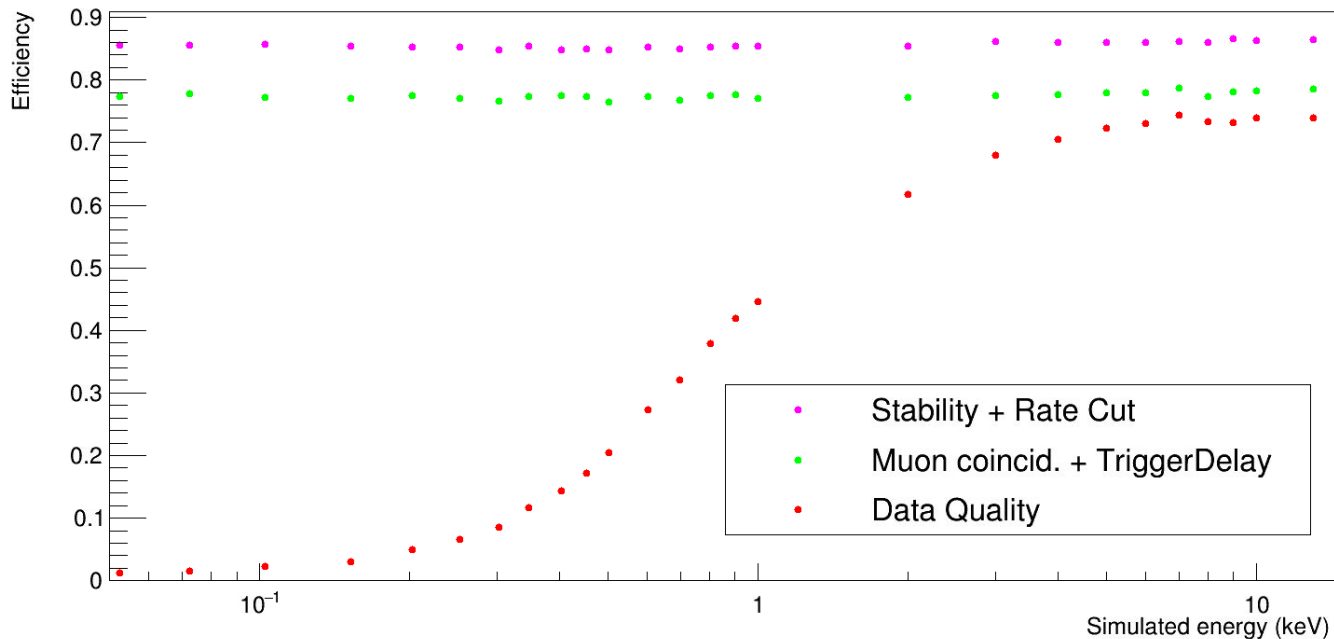


After data quality cuts



The neutron recoil events are not removed by the applied selection despite they have been defined on a dataset with very few neutron recoil event

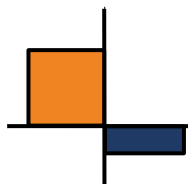
Defined as the survival probability of the signal events at a fixed simulated energy

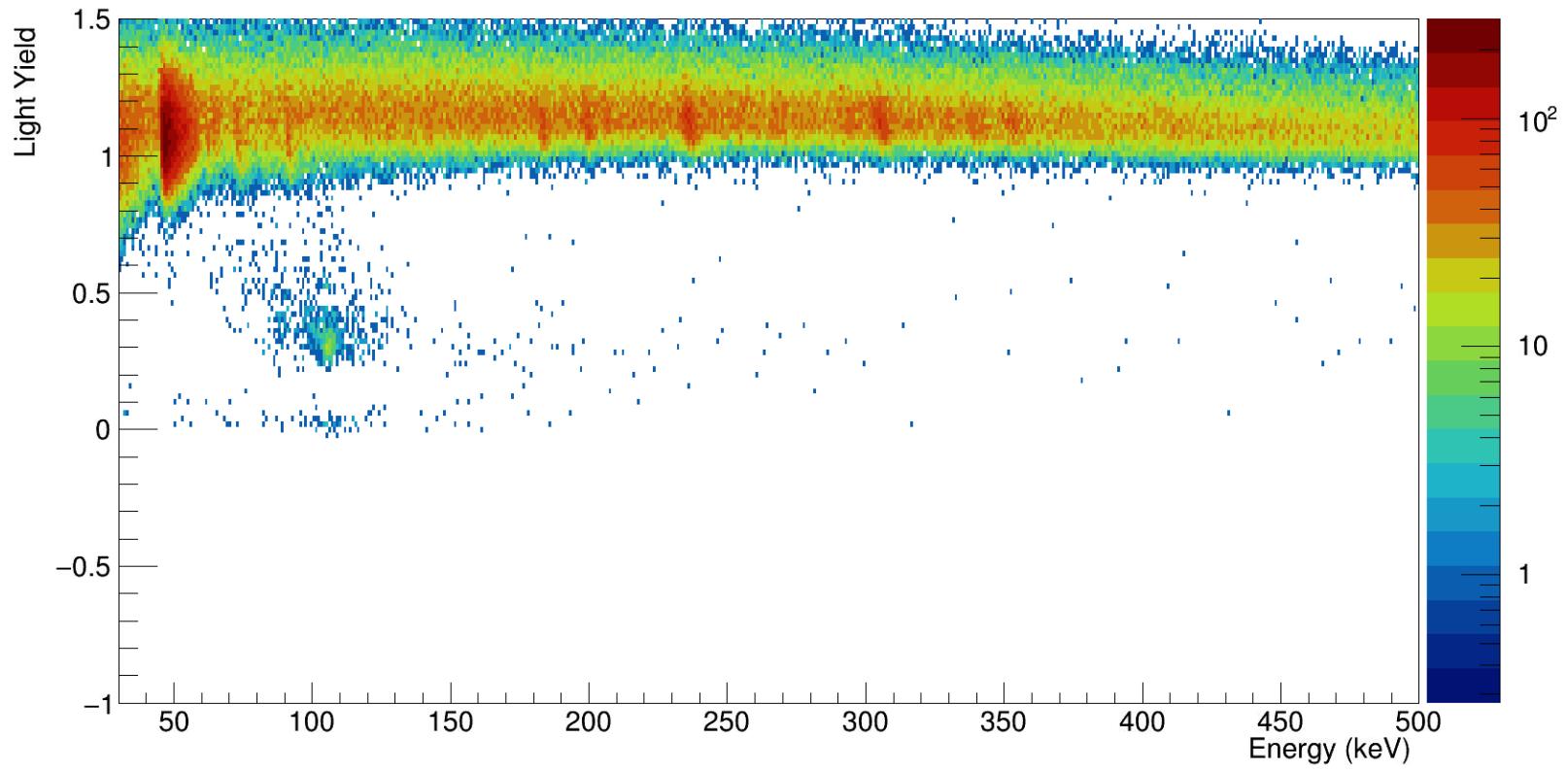


Simulated pulse = { Empty baseline + Scaled pulse template

To simulate nuclear recoils off Tungsten

Band fit





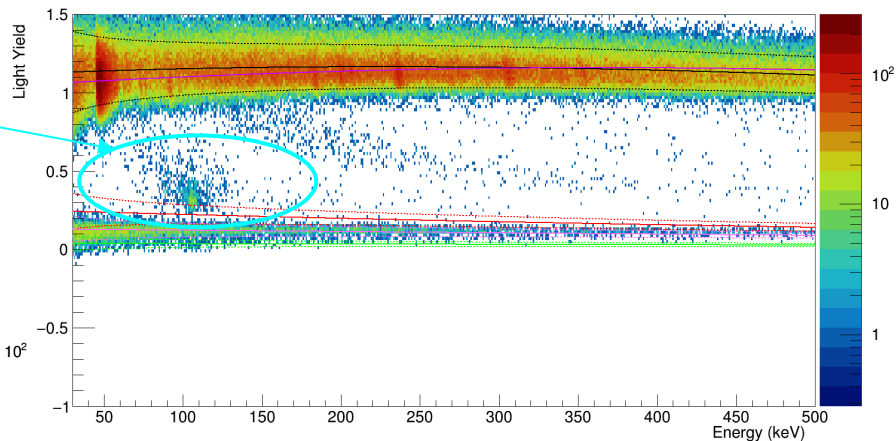
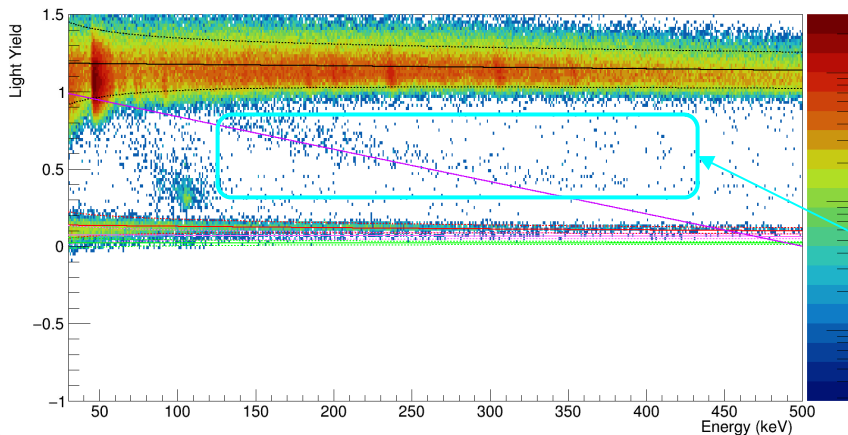
Band fit of NCal+Bck: problems

NR bands highly populated + general higher statistics help the fit convergence

BUT

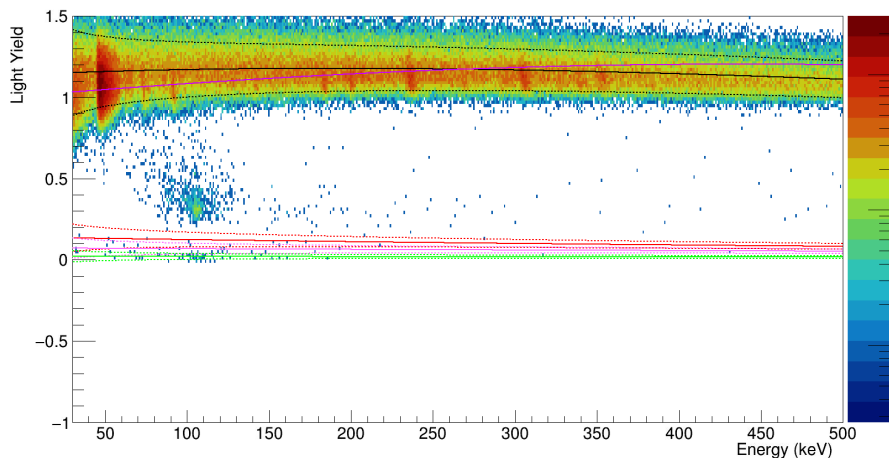
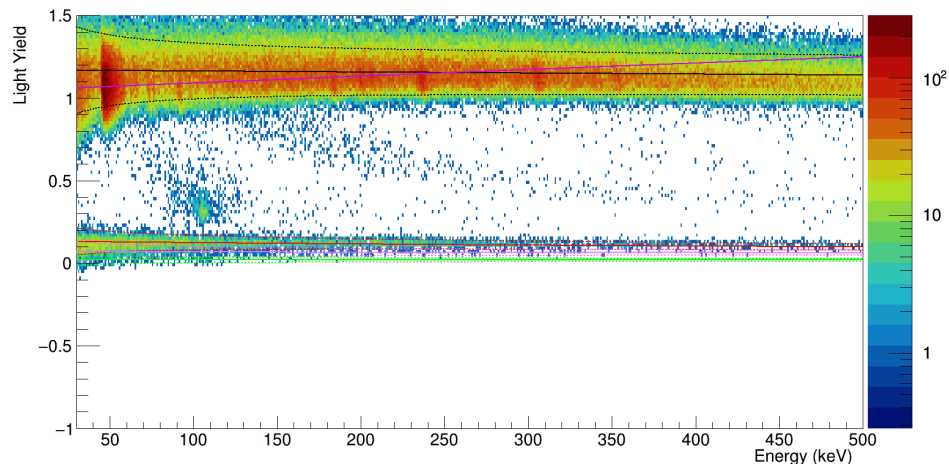
^{210}Po NR + inelastic scattering of neutrons off Tungsten nuclei are not recognised by the fit

The fitted Oxygen band is too high trying to “cover” the ^{210}Po NR events



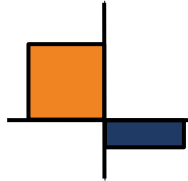
The fitted Gamma line is too low trying to “cover” the inelastic scattering of neutrons off Tungsten

NCal + Bck data



Bck data

Exclusion limit

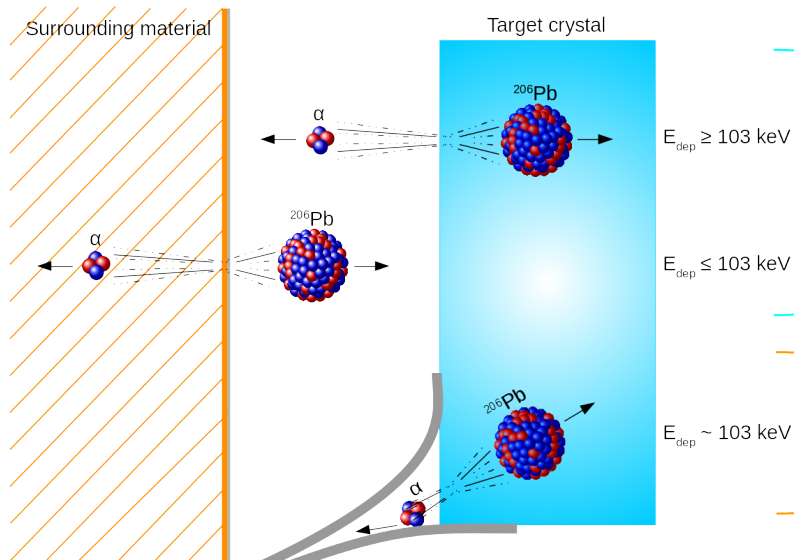


Results

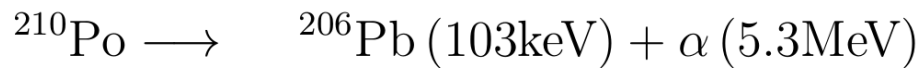
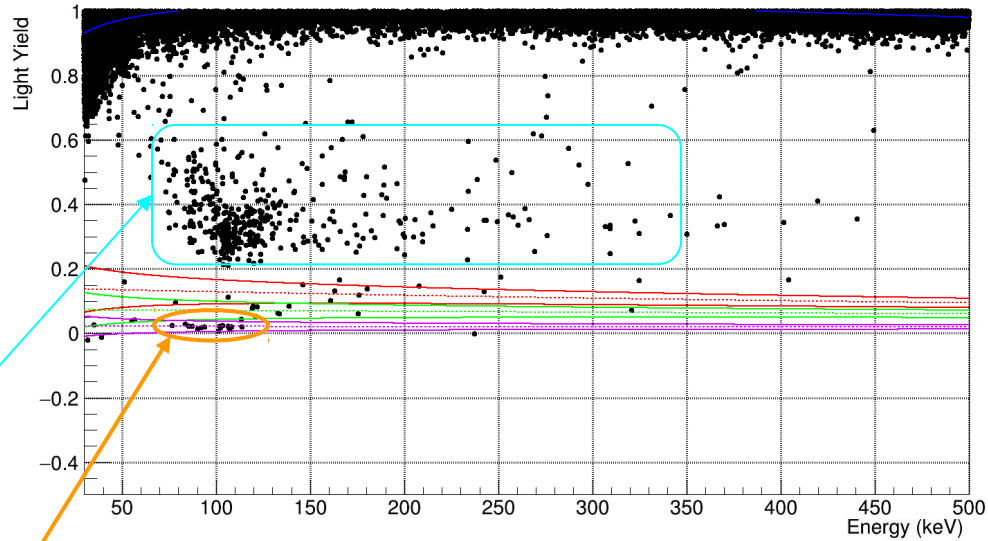
- In total 16 detector modules have been analysed
- A subset of 9 modules has been selected for the inelastic analysis based on background, noise, and live-time
- Exposure for a single module ~160 kg day

Results

^{210}Po recoils from surface radon contamination

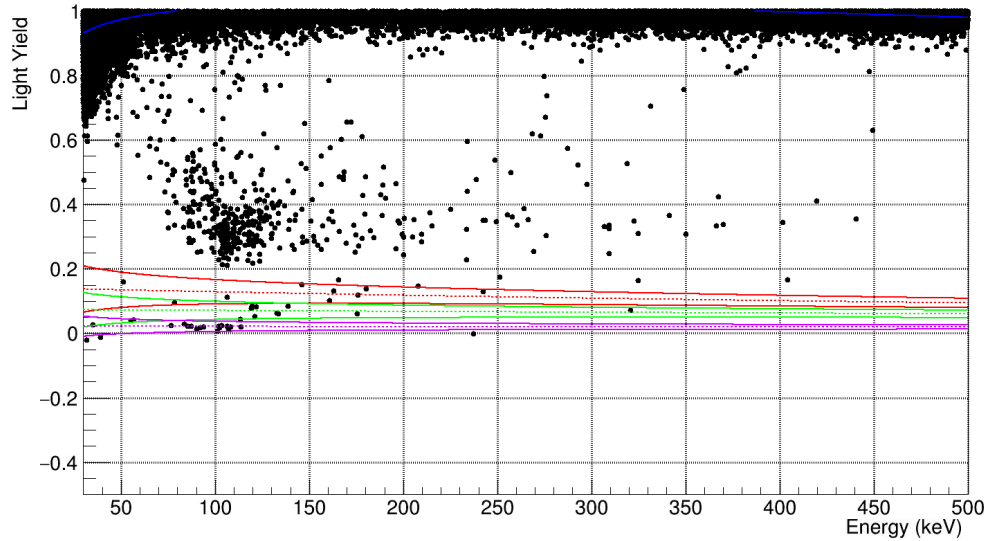


LY:E scatter plot of module Zora



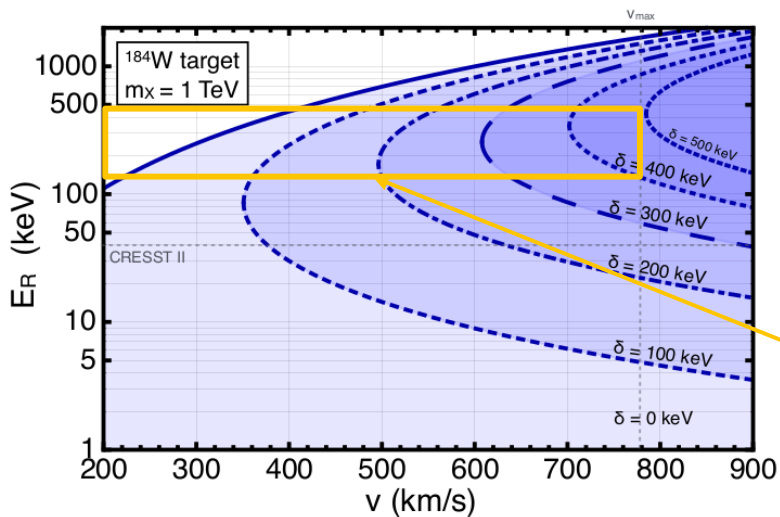
Results

LY:E scatter plot of module Zora



← Range adopted for the exclusion limit →

Probed kinematic phase space



Results

Extended Likelihood for D detectors

$$\mathcal{L}_{tot}^{ext}(\Theta | \mathbf{x}) = e^{-\mathcal{N}_{tot}(\Theta)} \prod_{d=1}^D \left[\prod_{i=1}^N \rho_d(x_i | \Theta) \right]$$

$$\text{with } \mathcal{N}_{tot}(\Theta) = \sum_{d=1}^D \left[\int_A \rho_d(\mathbf{x} | \Theta) d\mathbf{x} \right]$$

All parameters = interesting par. + nuisance par. $\longrightarrow \Theta = (\sigma_\chi, m_\chi, \delta, \theta)$

$$\ln \left(\mathcal{L}(\sigma_\chi, \hat{\boldsymbol{\theta}} | m_\chi, \delta, \mathbf{x}) \right) = \ln \left(\mathcal{L}(\hat{\sigma}_\chi, \hat{\boldsymbol{\theta}} | m_\chi, \delta, \mathbf{x}) \right) - \frac{Z^2}{2}$$

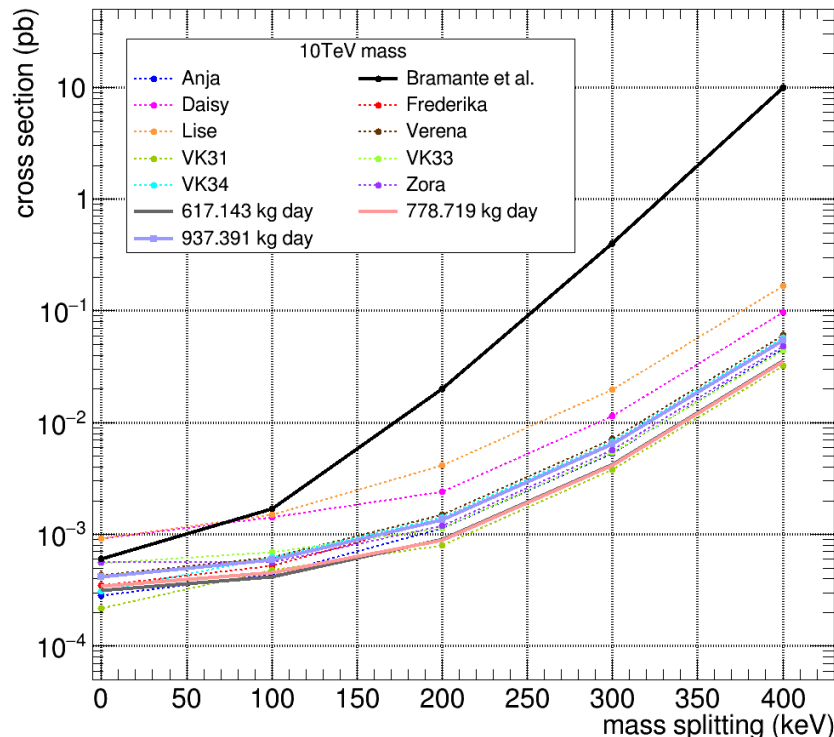
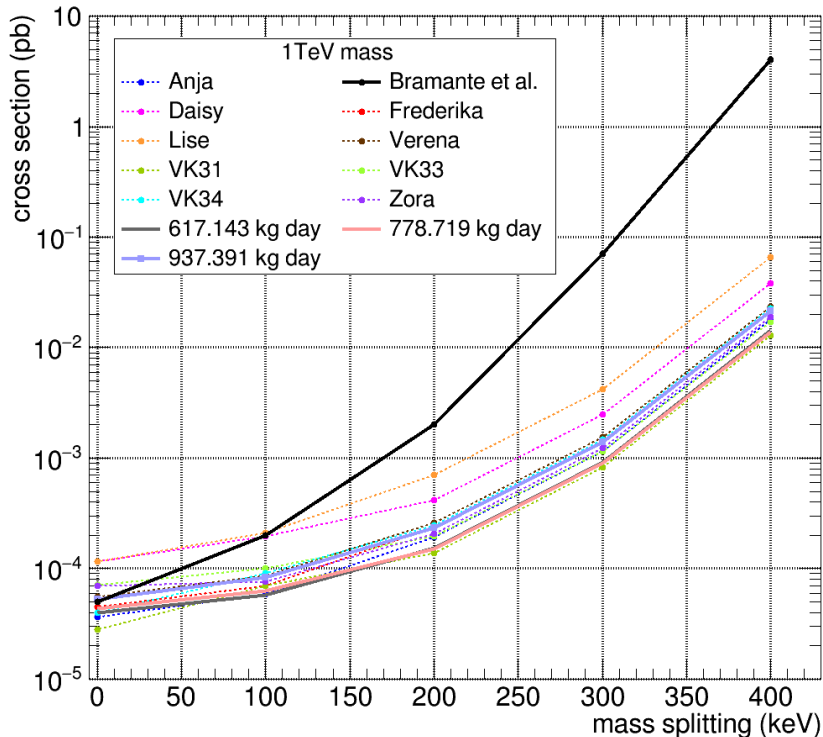
Profiled values

Best fit values

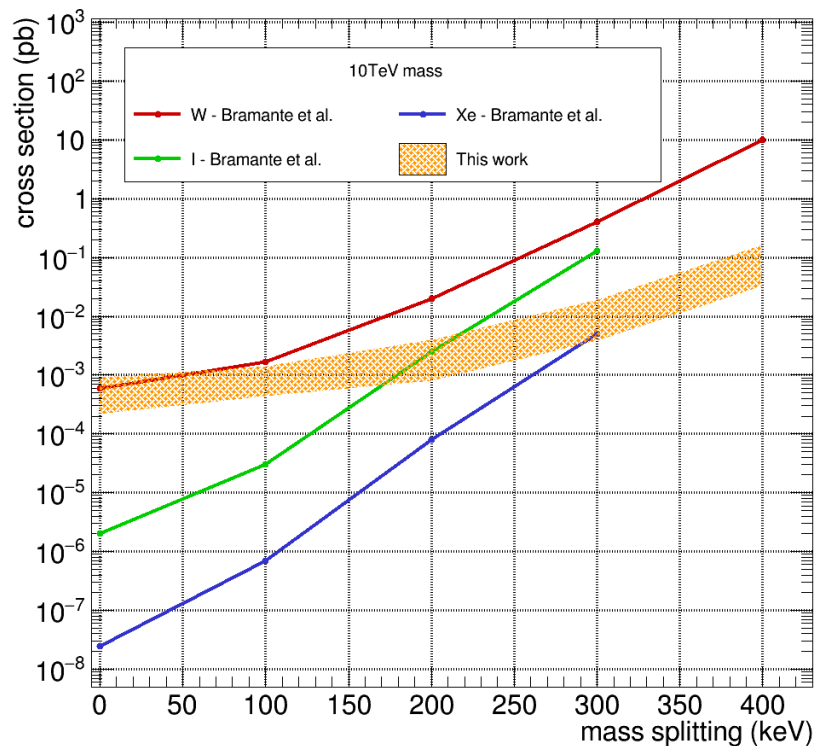
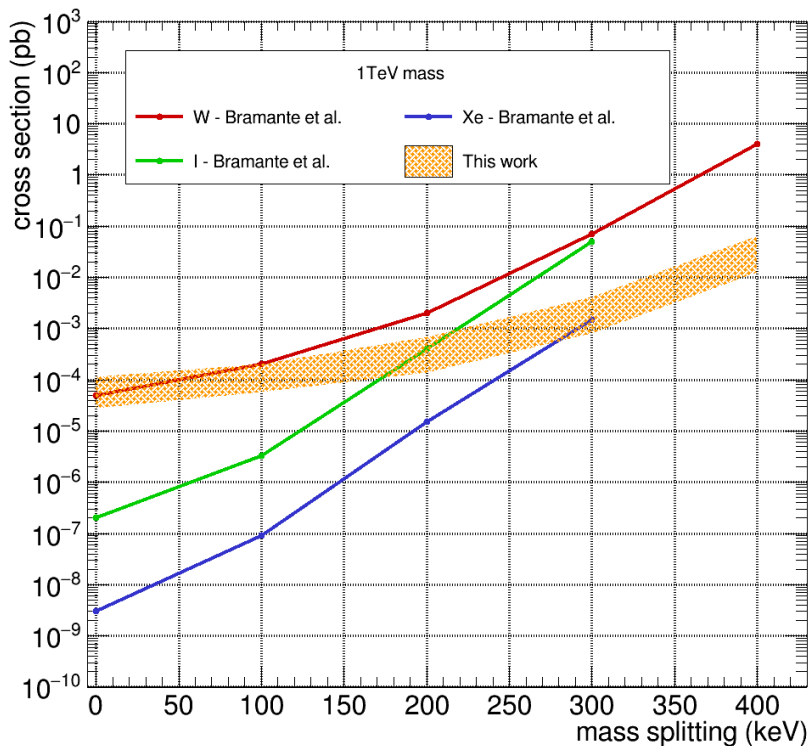
Significance of the limit

Z^2

Results

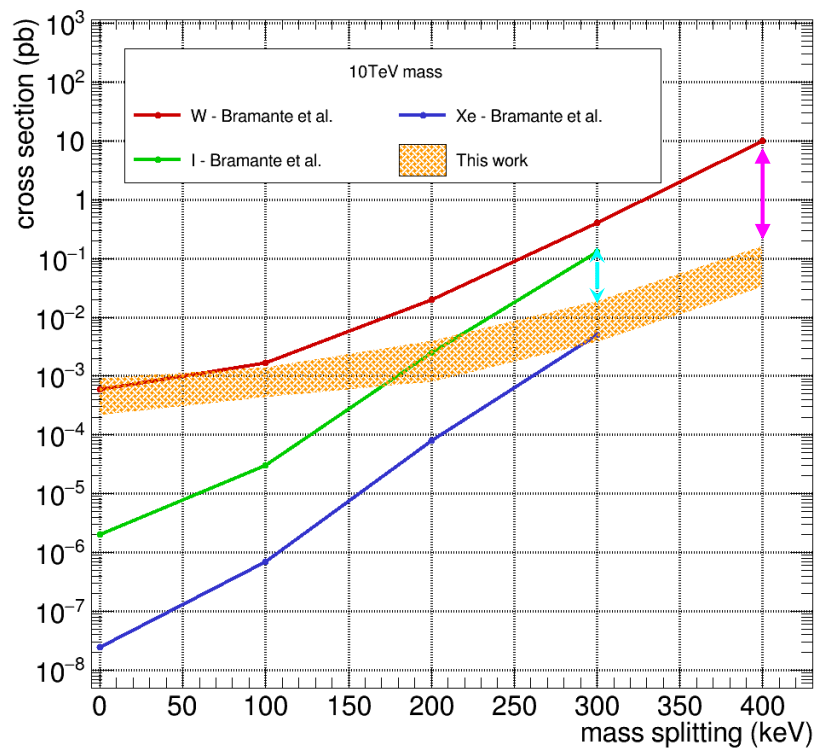
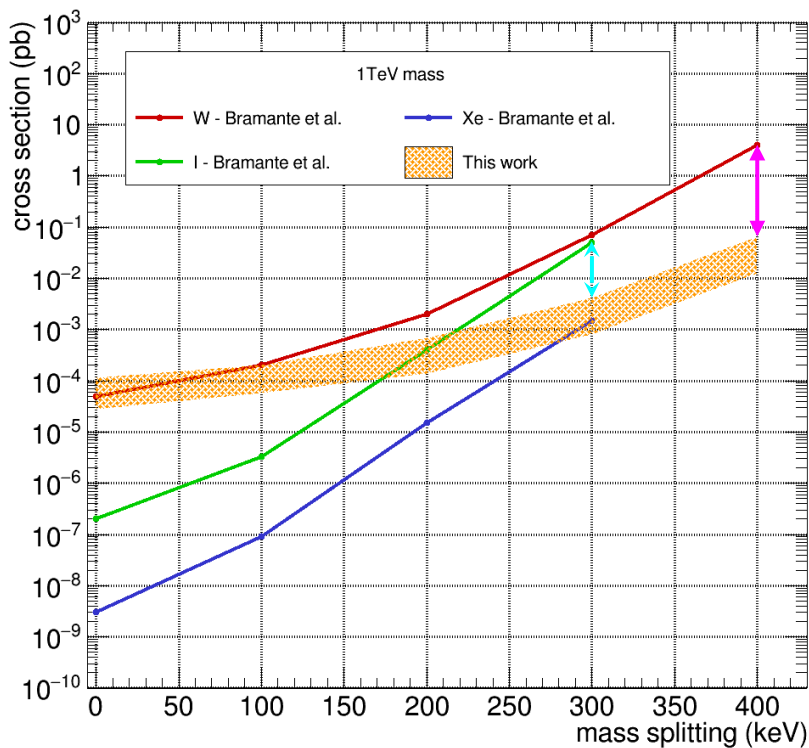


Results - comparison with other target elements



Estimated by Bramante et al. with following data: CRESST-II (W), PICO-60 (I),
[Phys. Rev. D 94, 115026 \(2016\)](https://arxiv.org/abs/1605.04673) LUX and PandaX 2016 (Xe)

Results - comparison with other target elements



→ Almost 2 orders of magnitude improvement with respect to Tungsten limit by Bramante

↔ Almost 1 order of magnitude improvement with respect to Iodine limit by Bramante

Conclusions

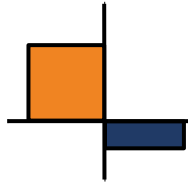
- Thanks to Tungsten CRESST detectors have been demonstrated to be very suitable for iDM search
- The exclusion limits for a DM mass of 1 TeV and 10 TeV and with a δ going from 0 to 400 keV have been obtained with a total exposure of ~ 900 kg day
- The resulting limits are the best limits ever obtained within this framework with Tungsten as target material
- For $\delta > 100$ keV the obtained limits exceeds the limit for Tungsten estimated by Bramante et al. with CRESST-II data
- Almost 2 orders of magnitude improvement at $\delta = 400$ keV with respect to the Tungsten limit estimated by Bramante et al.
- Almost 1 order of magnitude improvement at $\delta = 300$ keV with respect to the Iodine limit estimated by Bramante et al.

Improvement of the sensitivity for IDM signals:

- Increase of the exposure including more detectors in the analysis
- Improve the energy spectra description
 - Peaks in the dark bands
 - ^{210}Po recoil events
 - Inelastic scattering of neutrons off Tungsten

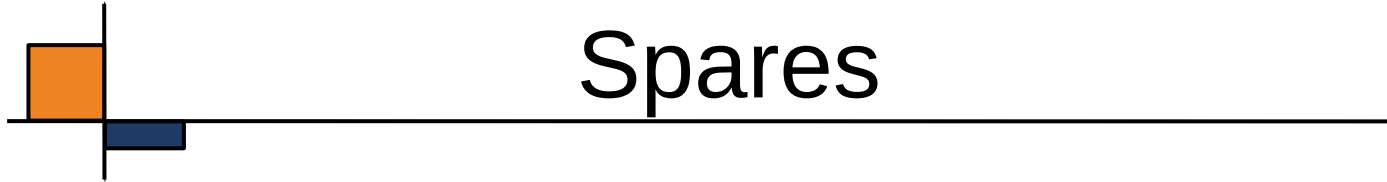
Finally to better estimate systematic uncertainties a MC simulation is needed.

Paper with this analysis is in preparation.



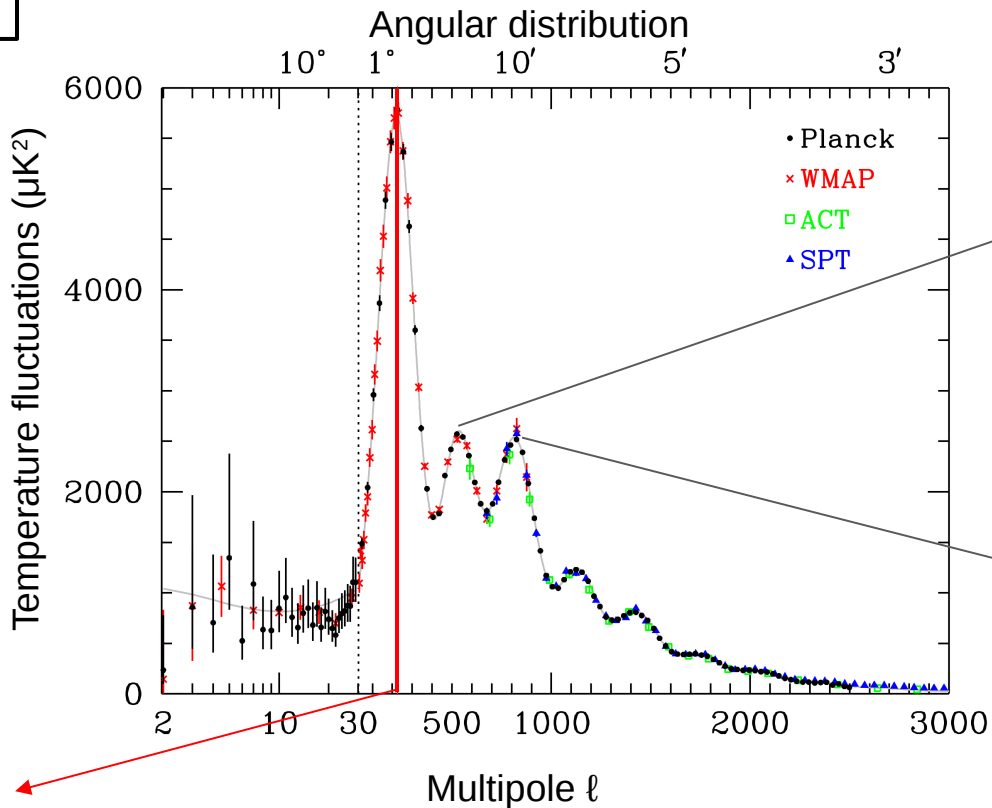
Thanks for the attention

Spares



Evidence for Dark Matter

CMB anisotropy

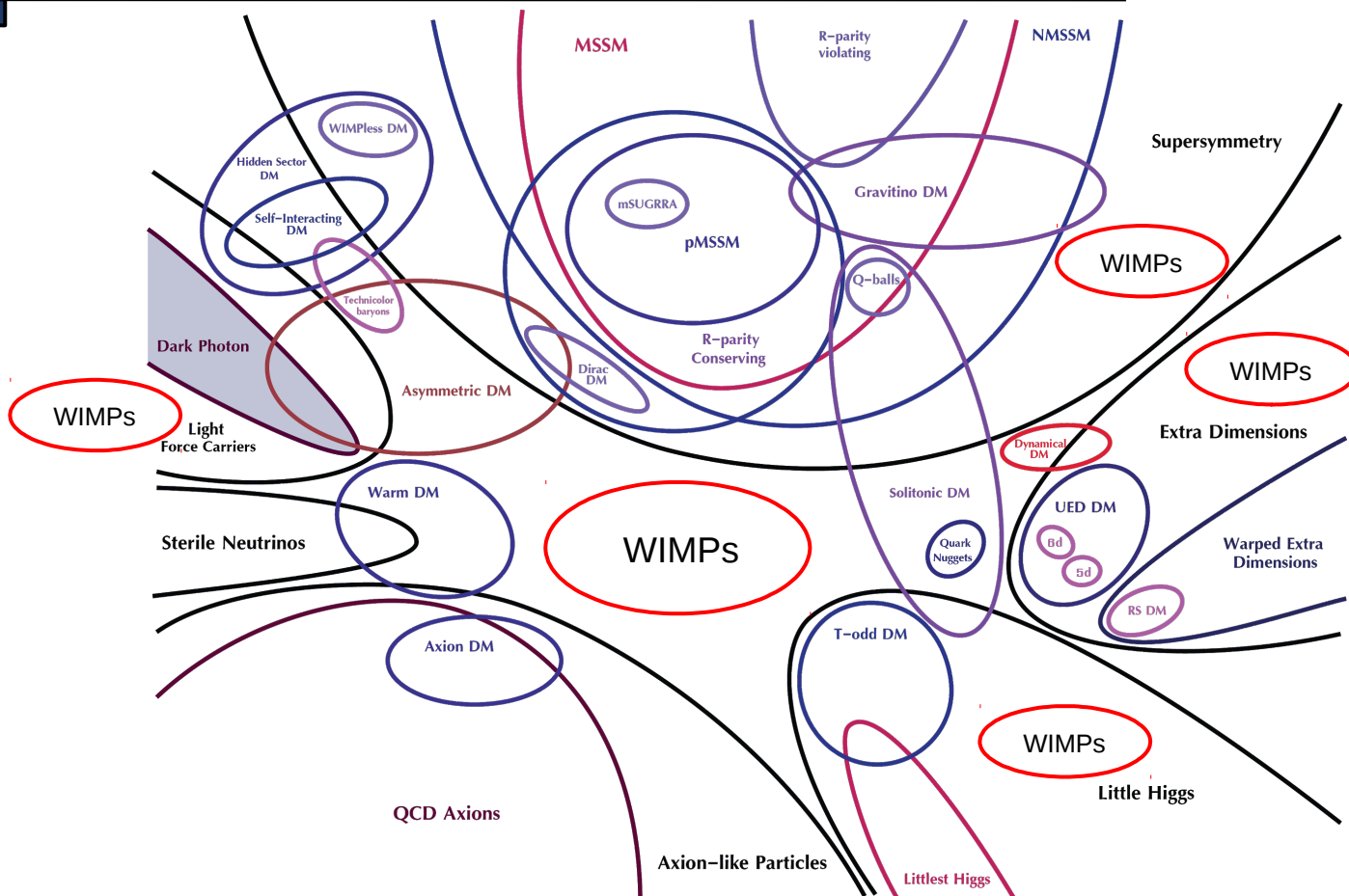


Amount of baryonic matter in the Universe

Amount of matter in the Universe

Curvature of the Universe

Models and Candidates



From T. Tait

Inelastic Dark Matter Scattering

$$f(\vec{v}, \vec{v}_e) = \frac{e^{-(v^2 + v_e^2 + 2v v_e \cos\theta)/v_0^2}}{N(v_0, v_{esc})}$$

$$\frac{d\sigma}{dE_R} = \frac{\sigma_n m_N}{v^2 2\mu_n^2} A^2 F_h^2(E_R)$$

$$\frac{dR}{dE_R dM} = n_\chi N_T \int_{v_{min}}^{v_{max}} v f(\vec{v}, \vec{v}_e) \frac{d\sigma}{dE_R} d^3v$$

$$v_{min} = \frac{1}{\sqrt{2E_R m_N}} \left(\frac{E_R m_N}{\mu} + \delta \right)$$

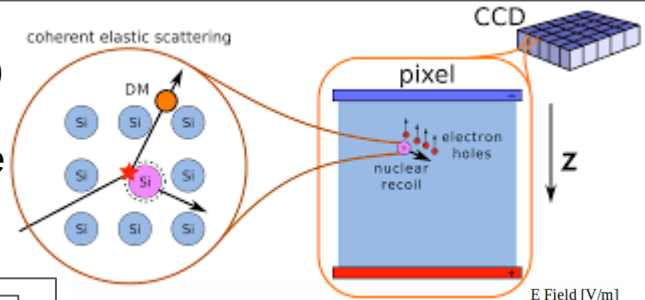
Experimental approaches for direct detection

Incoming particle with $v/c \sim 10^{-3} \Rightarrow$ DM mass in [100-1] GeV \Leftrightarrow NR energy in [0.1-100] keV

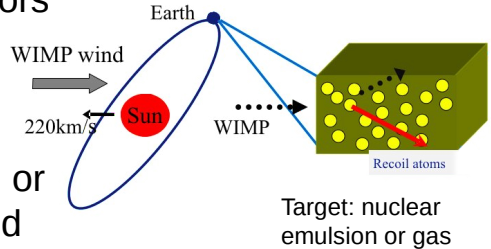
- Solid-state cryogenic detectors
- Noble liquids detectors
- Room temperature scintillating detectors
- Room temperature ionisation detectors
- Super-heated liquid detectors
- Directional detectors

silicon charged-coupled devices (CCDs) (DAMIC) spherical proportional counters filled with noble gas (NEWS-G)

Low Mass DM



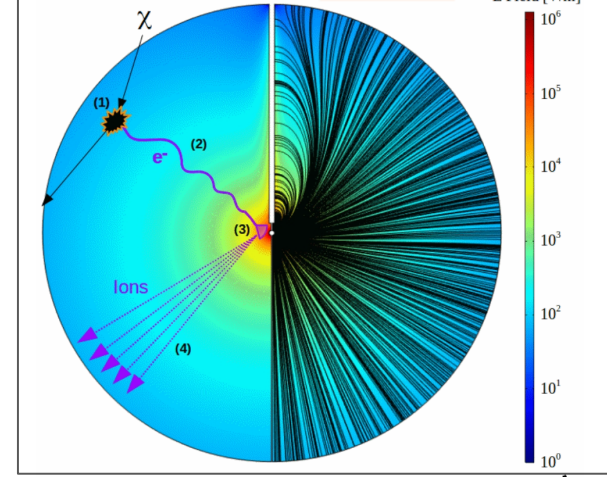
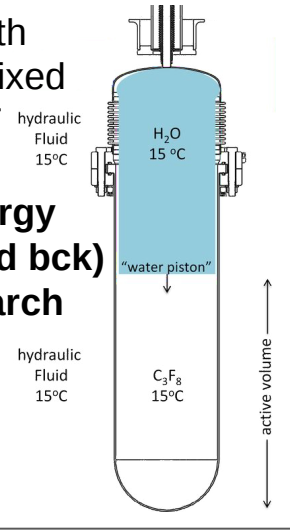
gas detectors (DRIFT, DMTPC, MIMAC, NEWAGE) or fine-grained nuclear emulsions (NEWSdm)



confirmation of the Galactic origin of a signal + probe of the region below the neutrino floor

devices with threshold fixed by P and T

Tuned energy region (and bck) for DM search



Detection of DM particles

- Colliders
- Indirect search
- Direct search

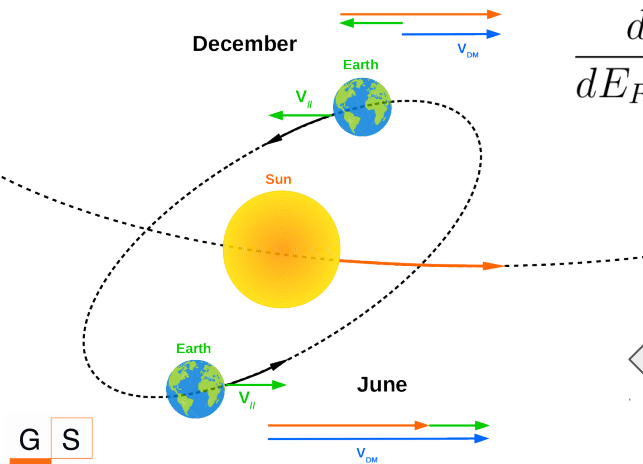
Basic assumption: DM particles are naturally produced during interaction of particle beams
 NB: collider searches cannot prove dark matter

Basic hypothesis: DM particles interact (weakly) via elastic and inelastic scattering with atomic nuclei or with electrons in the detector material

Search of annihilation or decay products of DM particles resulting in detectable species, especially gamma rays, neutrinos and antimatter particles

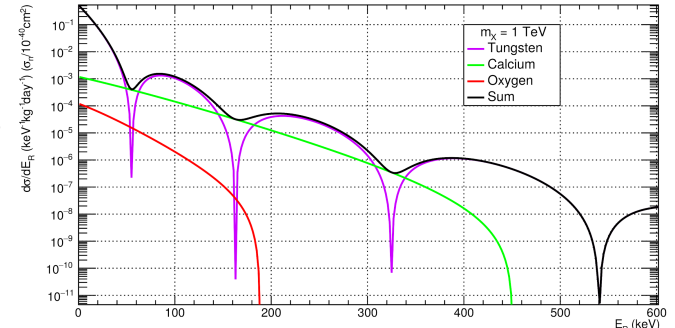
$$\frac{dR}{dE_R dM} = n_X N_T \int_{v > v_{min}} v f(\vec{v}, \vec{v}_e) \frac{d\sigma}{dE_R} d^3v \quad \text{with } v_{min} = \sqrt{\frac{E_R m_N}{2\mu^2}}$$

$$\frac{dR}{dE_R dM} = n_X N_T \int_{v_{min}}^{v_{max}} v f(\vec{v}, \vec{v}_e) \frac{d\sigma}{dE_R} d^3v \quad \text{with } v_{min} = \frac{1}{\sqrt{2E_R m_N}} \left(\frac{E_R m_N}{\mu} + \delta \right)$$



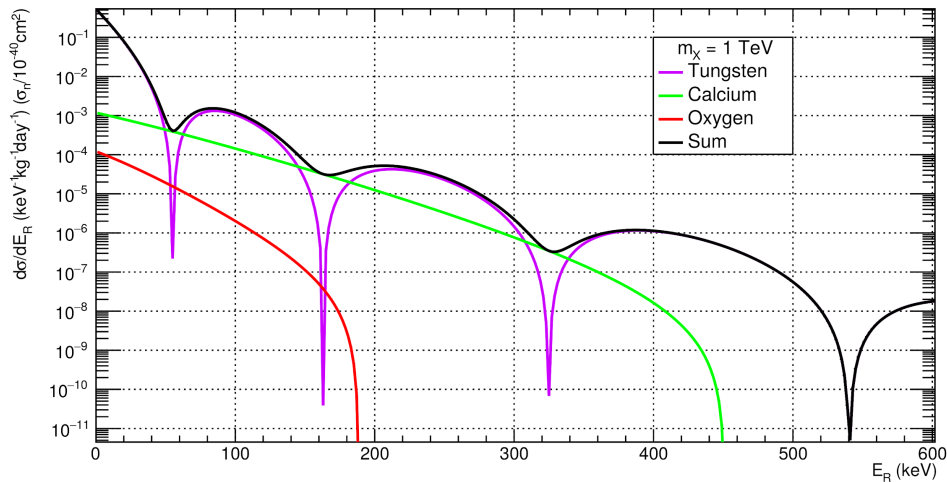
Expected spectrum

Annual modulation

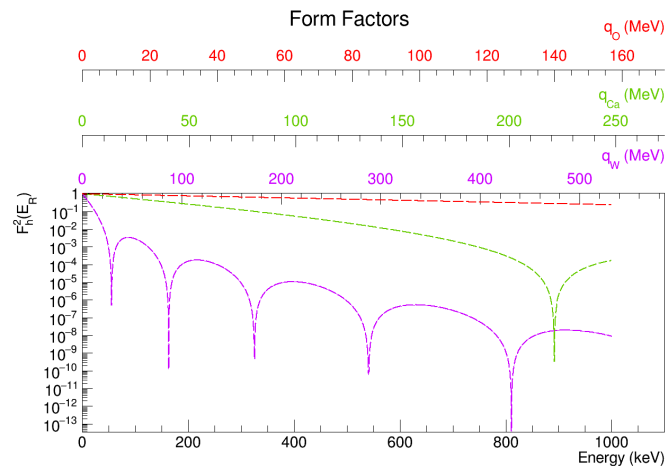


Elastic scattering of DM

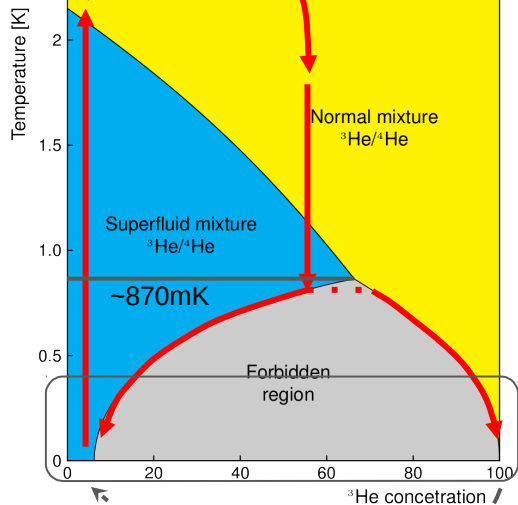
$$\frac{dR}{dE_R dM} = n_X N_T \int_{v>v_{min}} v f(\vec{v}, \vec{v}_e) \frac{d\sigma}{dE_R} d^3v \quad \text{with } v_{min} = \sqrt{\frac{E_R m_N}{2\mu^2}}$$



Expected spectrum in CaWO_4



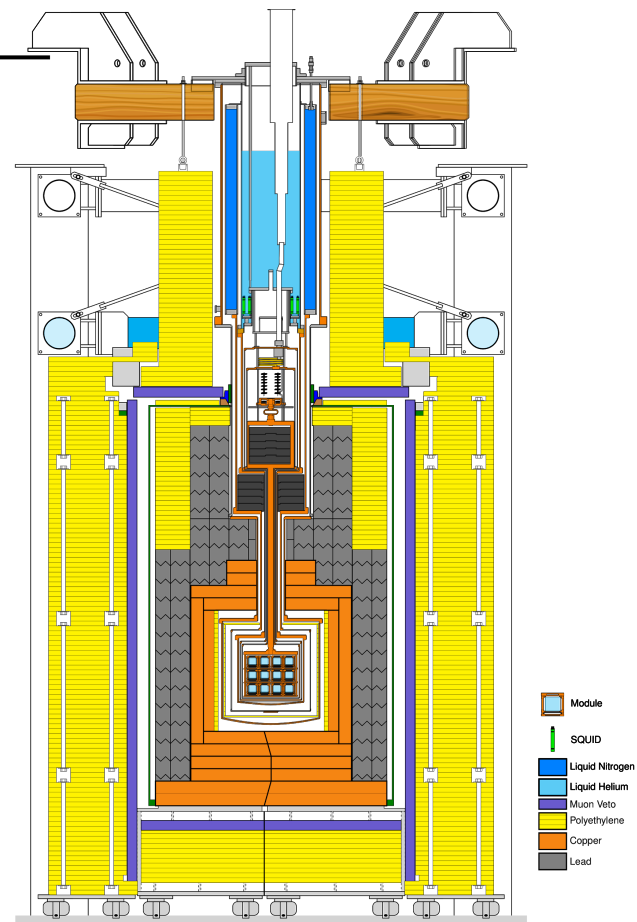
CRESST cryostat



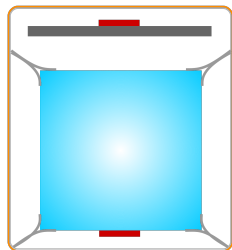
Due to different concentration ^3He crosses phase boundary cooling down the system

Working temperature $\sim 10\text{mK}$

- Dilution refrigerator circulating a mixture of 2 isotopes: ^3He and ^4He
- LNitrogen vapor and LHelium tanks
- Mixing chamber
- Additional lead to shield the detector from the dilution refrigerator
- Air dampers to attenuate external vibrations
- 5 thermal shield at decreasing temperatures
- “Cold finger”: copper rod 1.5 m long



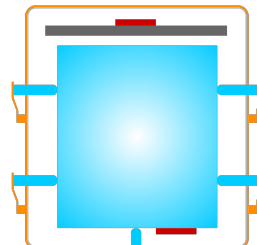
Run33 detector designs



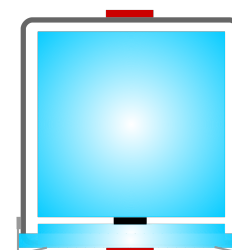
Std. design



Carrier design



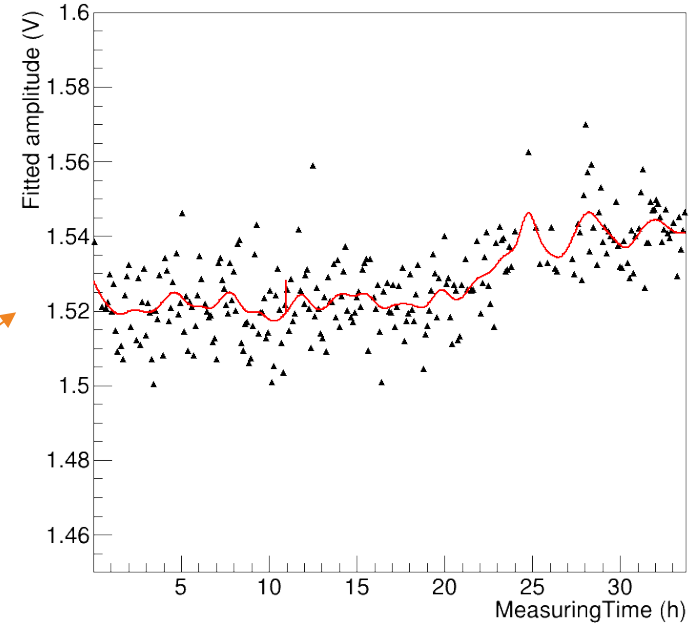
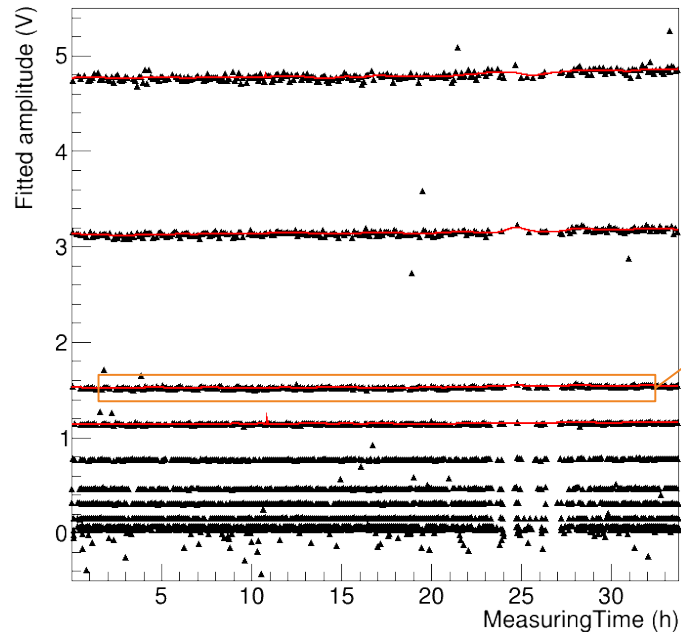
Stick design



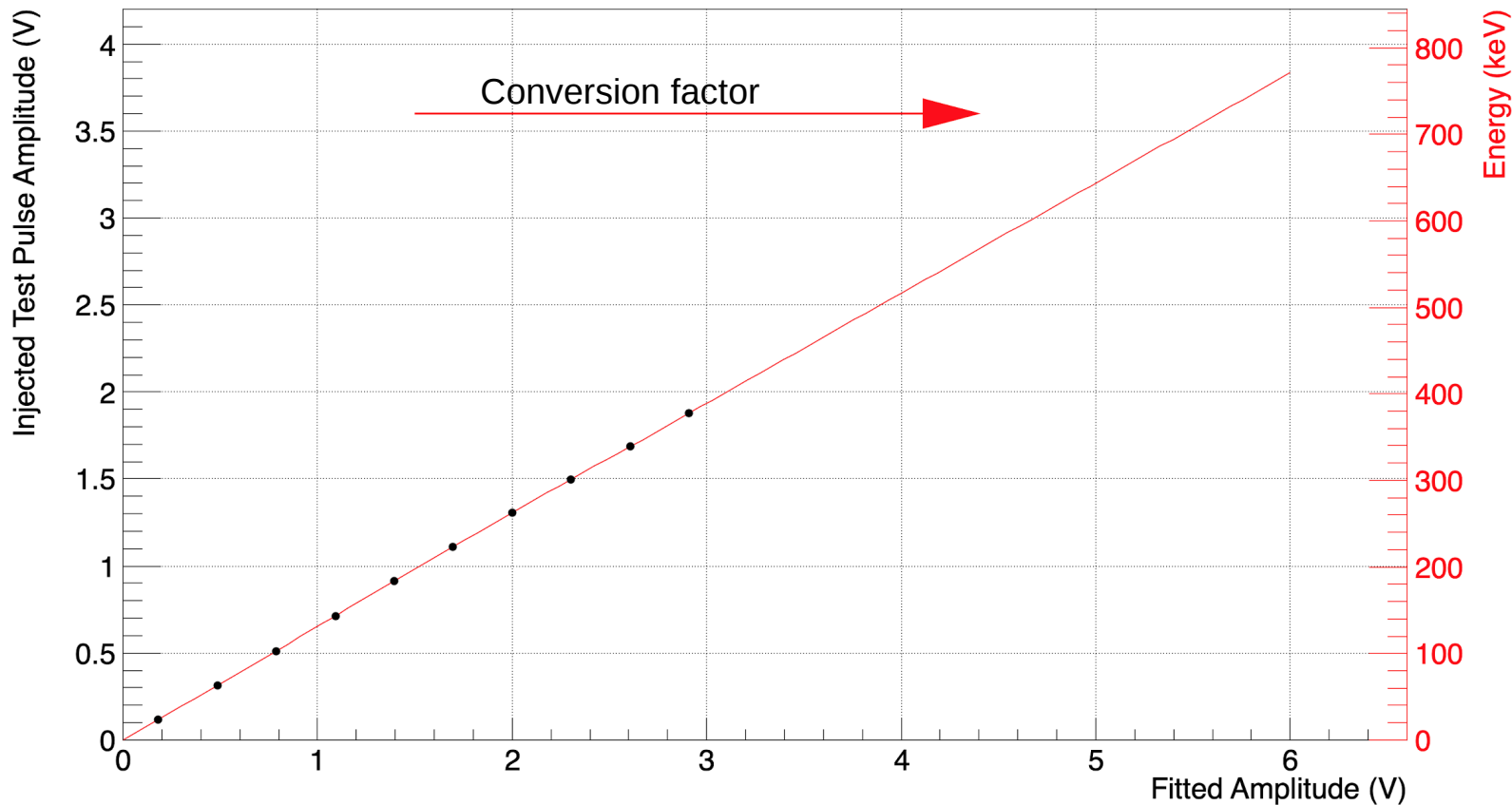
Beaker design

Correction of time-dependent effects

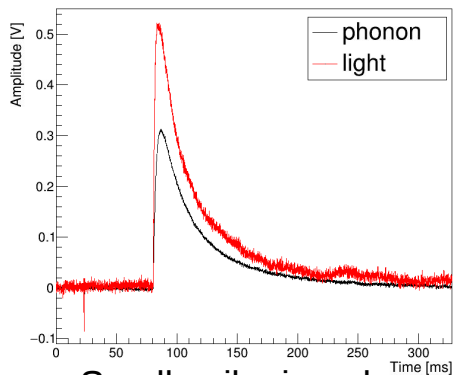
Heater pulses of small and varying amplitudes



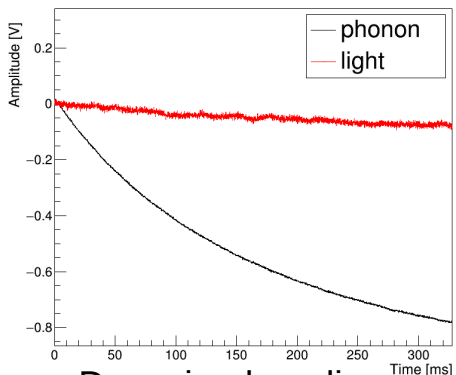
Energy calibration



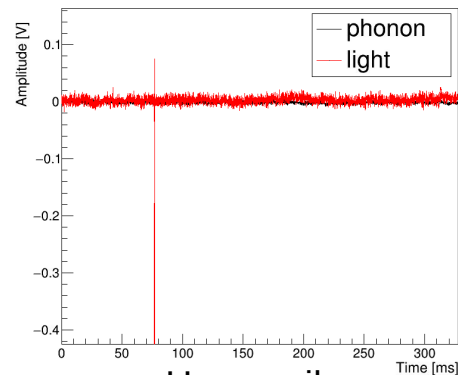
Data quality cuts



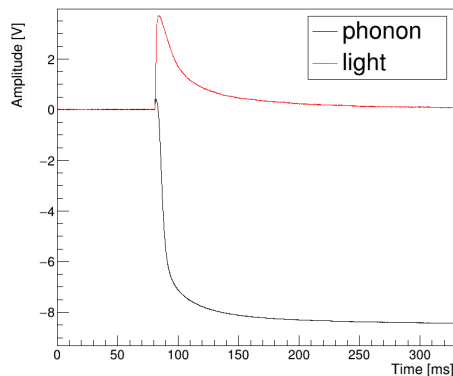
Small spike in pulse



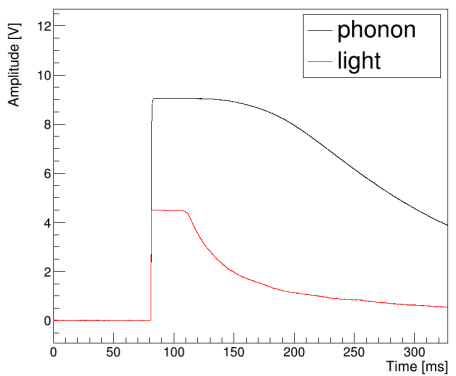
Decaying baseline



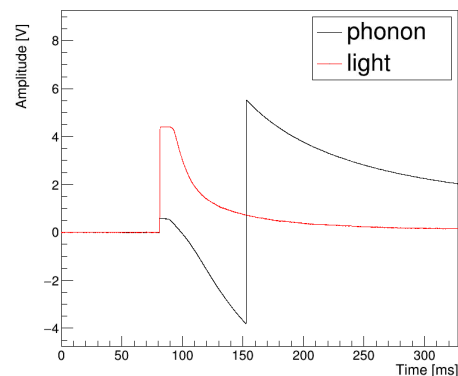
Huge spike



Flux quantum loss



Not recovered event



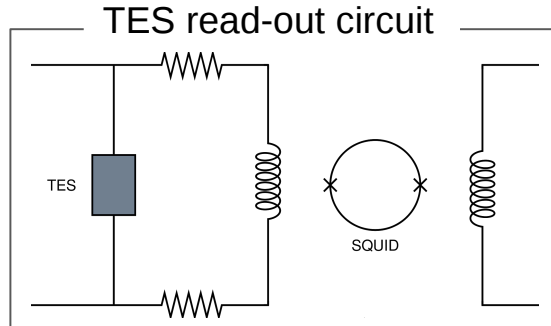
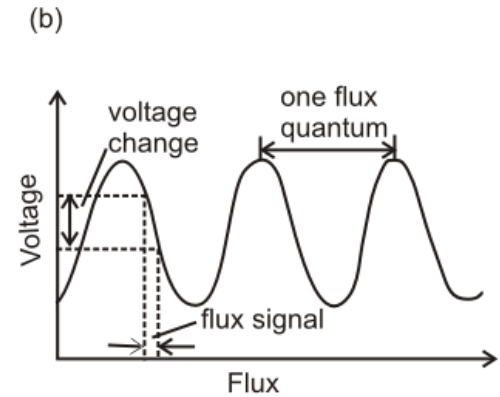
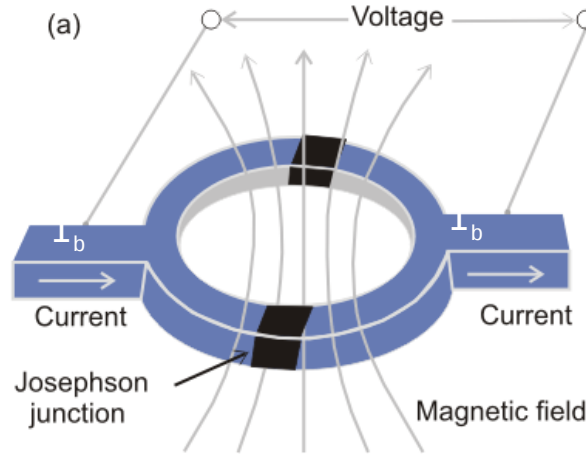
SQUID reset

Superconducting Quantum Interference Devices

Very sensitive magnetometer used to measure extremely subtle magnetic fields, based on superconducting loops containing Josephson junctions

superconducting rings can enclose magnetic flux only in multiples of a universal constant called the flux quantum, $\Phi_0 = h/2e = 2.07 \times 10^{-15}$ Wb

High sensitivity!

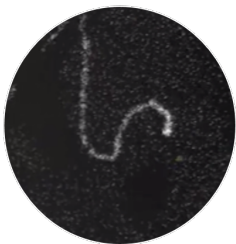


Flux locked in one loop by a feedback circuit. If the signal grows too fast the SQUID change loop and therefore the baseline level is different

Particle identification

$$QF^X(E_{\text{dep}}) = \frac{\text{Light produced by X when depositing } E_{\text{dep}}}{\text{Light produced by } \gamma \text{ when depositing } E_{\text{dep}}}$$

Particle tracks in a cloud chamber



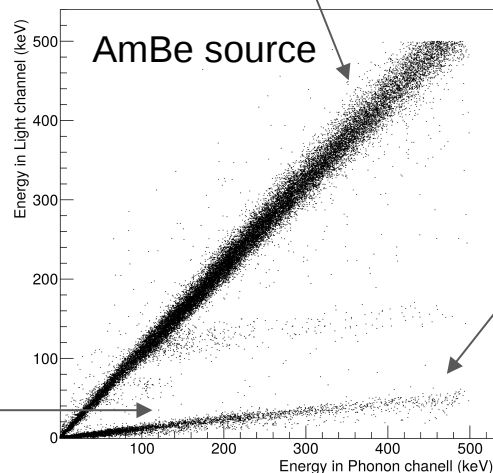
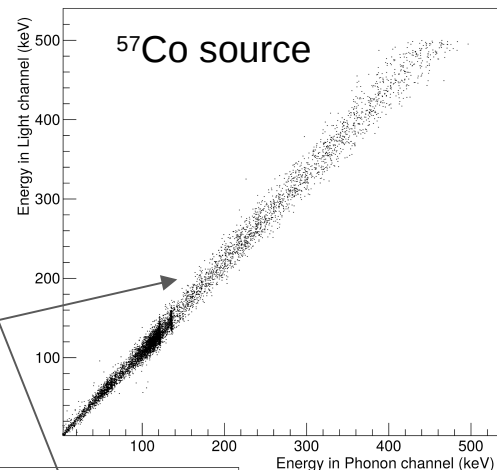
Beta particle / Electron



Alpha particle

Saturation of the scintillation centers

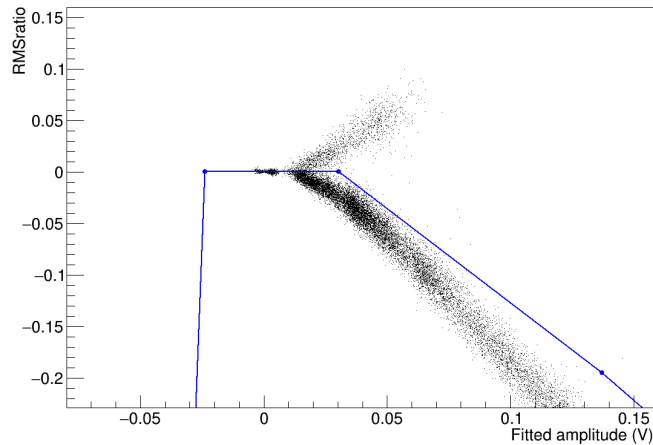
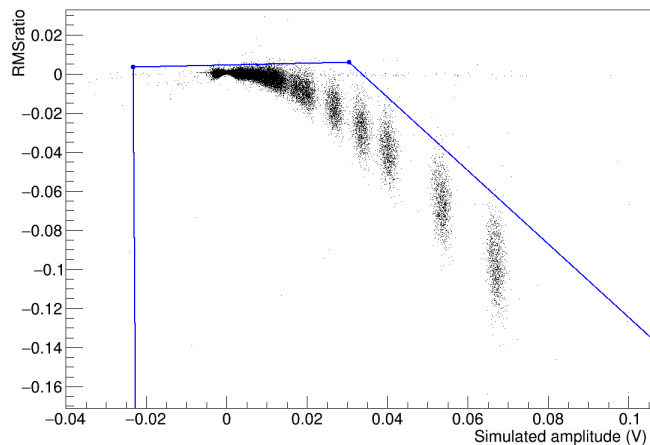
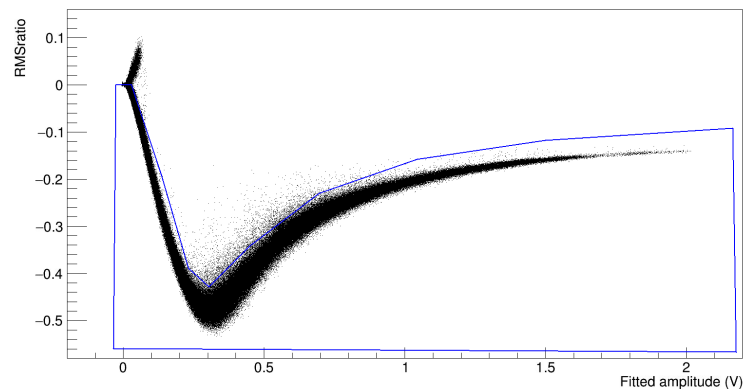
e/ γ band with slope set to 1 by construction



NR events with lower slope due to QFs

Carrier cut

$$\text{RMSratio} = \frac{\text{RMS}^a - \text{RMS}^c}{\text{RMS}^a + \text{RMS}^c}$$



η factor

$$E := \eta E + (1-\eta)E = \eta E_l + (1-\eta)E_p$$

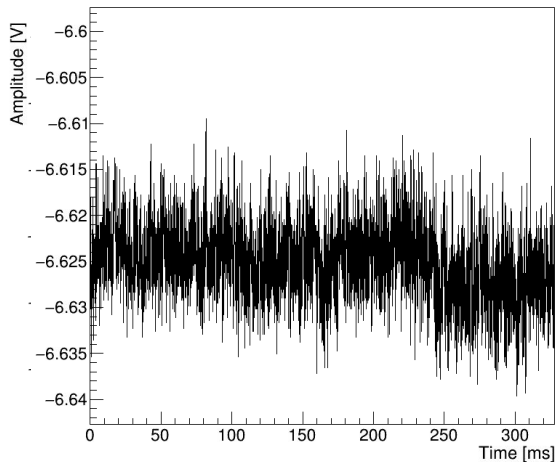
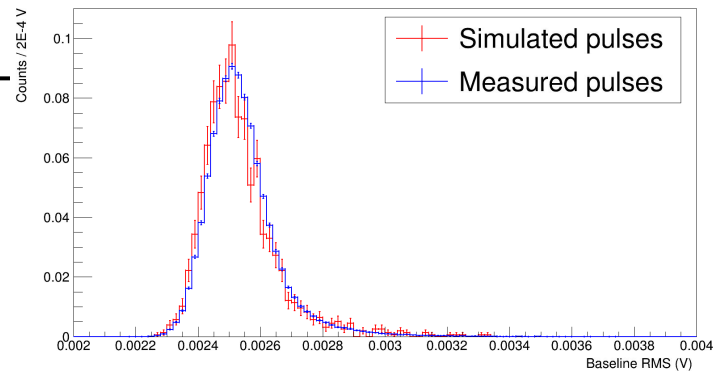
Always true
 η = scintillation efficiency

Due to the calibration procedure

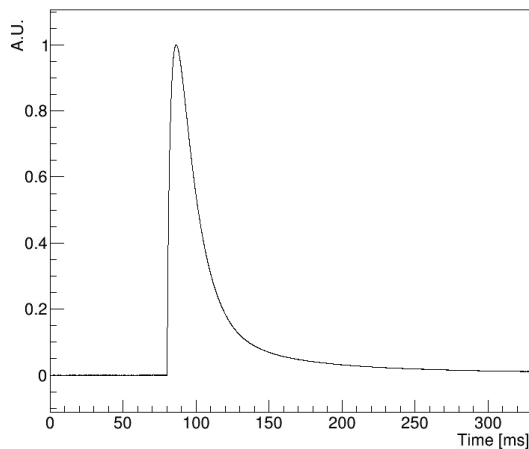
Consider a 122 keV incident $\gamma \rightarrow E = 122$ keV
Energy axis calibration $\rightarrow E_l = 122$ keV_{ee} and $E_p = 122$ keV_{ee}

$$LY = E_l / E_p \leftrightarrow E_l = LY E_p \Rightarrow E = \eta LY E_p + (1-\eta)E_p = E_p - \eta(1-LY)E_p \Rightarrow E = [1 - \eta(1-LY)] E_p$$

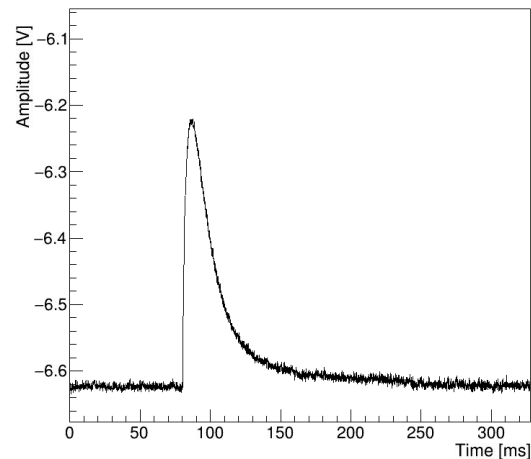
Simulated pulses



+



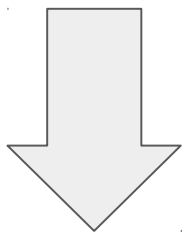
=



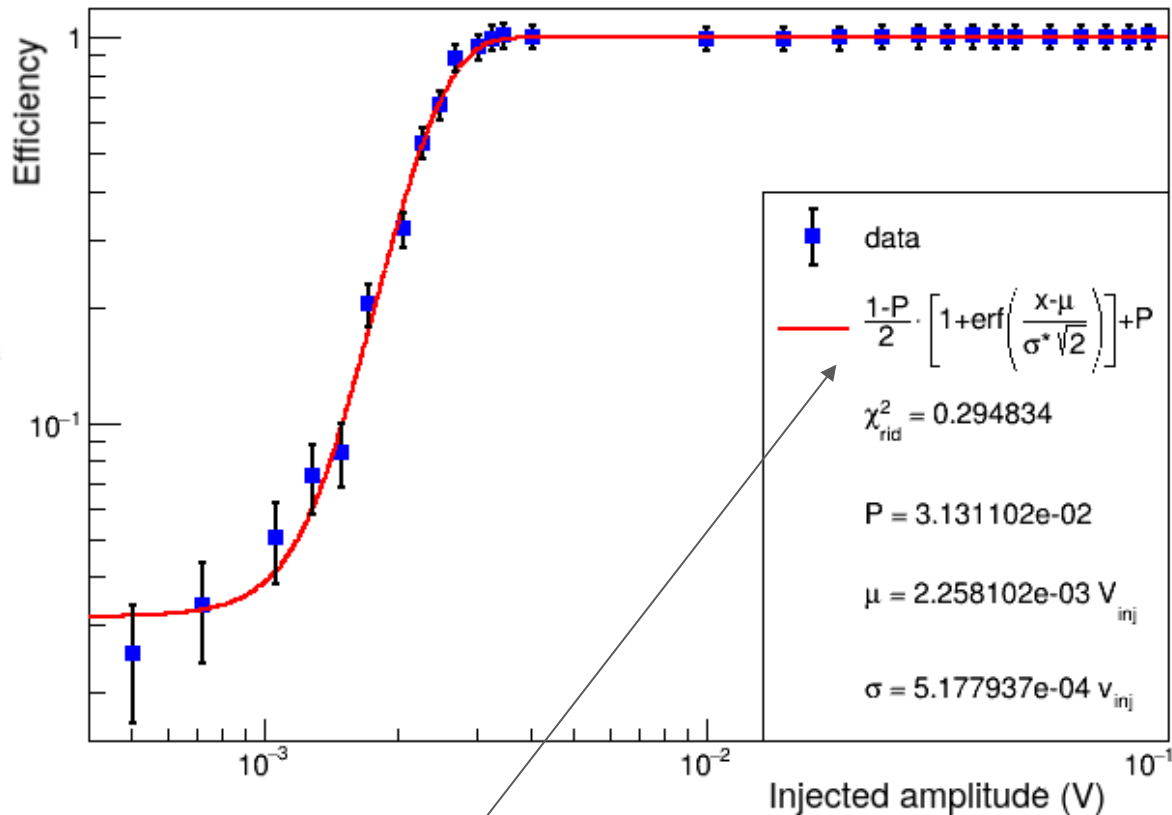
Trigger threshold

Number of injected pulses of
different amplitude firing the trigger

Number of pulses injected at
10V and firing the trigger

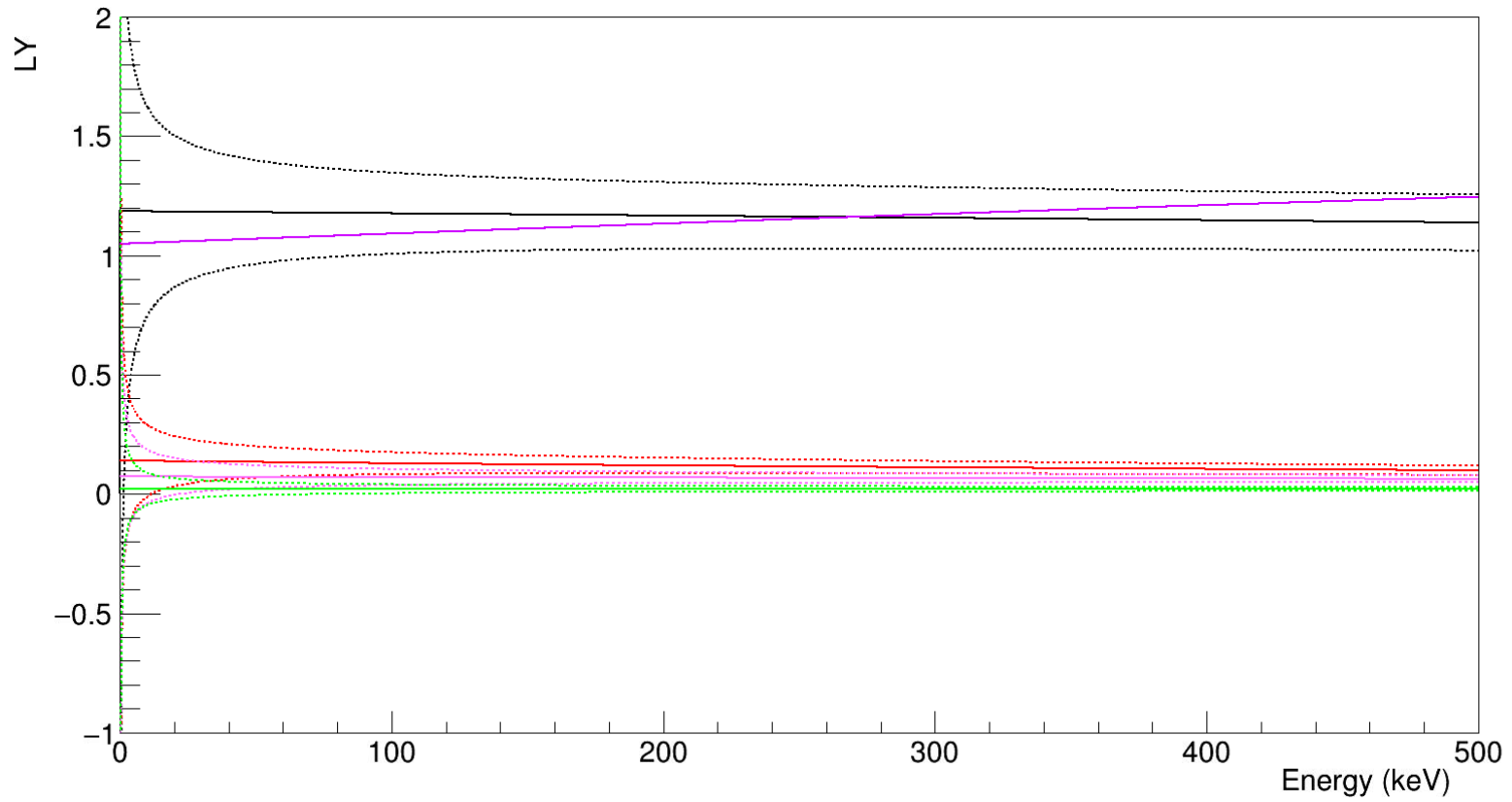


Each point is Poissonian
and not binomial
distributed



The P parameter accounts for the pedestal

Band fit



LY Bands

First approximation

$$L_{e^-}(E) = (L_0 E + L_1 E^2) \left[1 - L_2 \exp\left(-\frac{E}{L_3}\right) \right]$$

Non-proportionality effect

$$L_\gamma(E) = L_{e^-}(E [Q_{\gamma,1} + EQ_{\gamma,2}])$$

To account for ys interaction:
Multiple electrons with energy smaller than the one of the incident γ are produced

$$\rho_{excess}(E, L) = A_{excess} \exp\left(-\frac{E}{\lambda_{excess}}\right) \cdot$$

$$\left\{ \frac{1}{2\Delta_{excess}} \exp\left(-\frac{L}{\Delta_{excess}} + \frac{(\sigma_{L,e})^2}{2\Delta_{excess}^2}\right) \cdot \left[1 + \operatorname{erf}\left(\frac{L}{\sqrt{2}\sigma_{L,e}} - \frac{\sigma_{L,e}}{\sqrt{2}\Delta_{excess}}\right) \right] \right\}$$

First approximation

$$L_x(E) = (L_0 E + L_1 E^2) \cdot \epsilon \cdot \text{QF}_x \cdot \left[1 + f_x \exp\left(-\frac{E}{\lambda_x}\right) \right]$$

Crystal specific

Non-proportionality effect

Energy resolution & band width

Energy resolution of a single channel

$$\sigma_{BLN}(keV) = CPE(keV/V) \cdot TPA(V) \cdot \frac{\sigma^{fit}(V)}{\mu^{fit}(V)}$$

$$\sigma_P(E) = \sqrt{\sigma_{P,0}^2 + \sigma_{P,1}E}$$

$$\sigma_L(L) = \sqrt{\sigma_{L,0}^2 + S_1L + S_2L^2}$$

Parametrization of the energy resolution of phonon and light detectors

LY band width of the x-th species

$$\sigma_x = \sqrt{\sigma_L(L) + \frac{dL_x}{dE}(E) \sigma_P(E)}$$

Energy spectra

$$\frac{dN_e}{dE} = P_0 + P_1 E + F_e \exp\left(-\frac{E}{D_e}\right) \quad \leftarrow \text{Electron spectrum}$$

$$\frac{dN_{\beta\gamma,x}}{dE} = \mathcal{G}(E, \sigma_P(E)) * [C_{\beta\gamma,x} \mathcal{T}(E, E_{\beta\gamma,x}^0, Q_{\beta\gamma,x})] \quad \leftarrow \text{Beta-gamma peaks spectrum}$$

$$\mathcal{T}(E, E_{\beta\gamma,x}^0, Q_{\beta\gamma,x}) = \frac{2}{E_{\beta\gamma,x}^0 Q_{\beta\gamma,x}} \begin{cases} E_{\beta\gamma,x}^0 - \frac{E_{\beta\gamma,x}^0}{Q_{\beta\gamma,x}} (E - E_{\beta\gamma,x}^0) & \text{if } E_{\beta\gamma,x}^0 < E < E_{\beta\gamma,x}^0 + Q_{\beta\gamma,x} \\ 0 & \text{otherwise} \end{cases}$$

$$\frac{dN_{\gamma,x}}{dE} = \frac{C_{\gamma,x}}{\sqrt{2} * \pi \sigma_P(M_x)} \exp\left(-\frac{(E - M_x)^2}{2(\sigma_P(M_x))^2}\right) \quad \leftarrow \text{Gamma peaks spectrum}$$

$$\frac{dN_{n,x}}{dE} = A_{n,x} \exp\left(-\frac{E}{E_{n,x}^{decay}}\right) \quad \leftarrow \text{Neutron spectrum}$$

Density functions

$$\rho_x(E, L) = \frac{dN_x}{dE}(E) \cdot \frac{1}{\sqrt{2\pi}\sigma_x(E)} \cdot \exp\left(-\frac{[L - L_x(E)]^2}{2\sigma_x^2(E)}\right)$$

$$\rho_{ncal} = \rho_e + \rho_\gamma + \rho_{ns}$$

Neutron signals
scattering off nucleus X

$$\rho_{bck} = \rho_e + \rho_\gamma + \rho_{nb} + \rho_\chi$$

Neutron background
scattering off nucleus X

With ρ_{ns} , ρ_{nb} , ρ_χ given by the sum
of the contribution of Oxygen,
Calcium and Tungsten

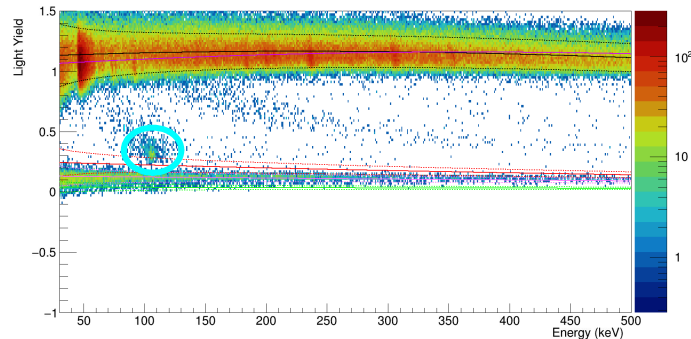
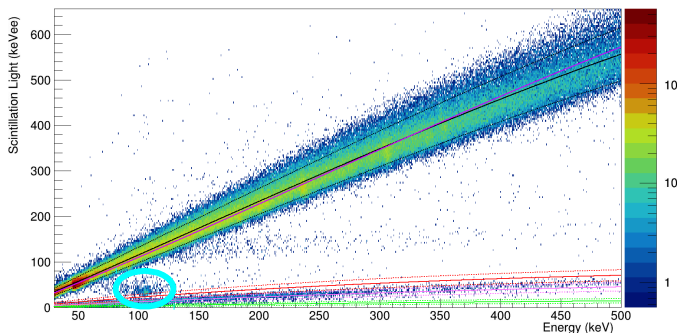
Band fit of NCal+Bck: problems

NR bands highly populated + general higher statistics help the fit convergence

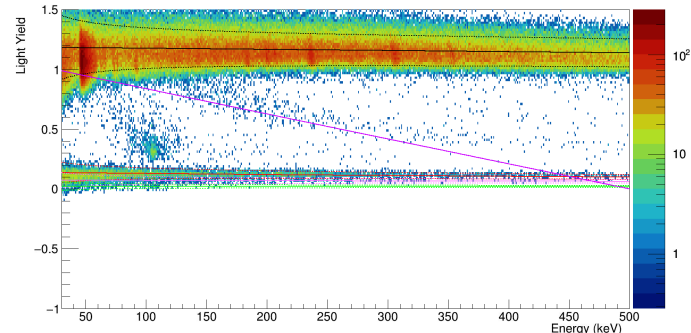
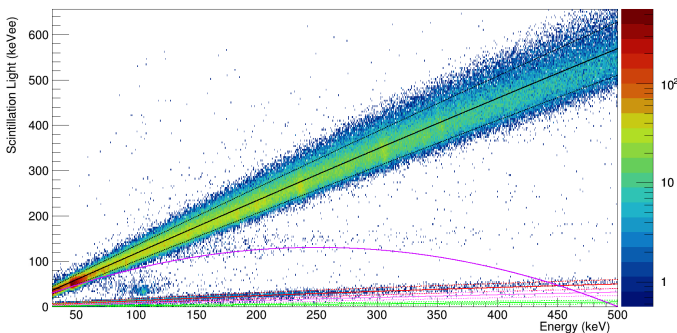
BUT

Polonium NR + inelastic scattering of neutrons off Tungsten nuclei are not recognised by the fit

The fitted Oxygen band is too high trying to “cover” the Polonium NR events

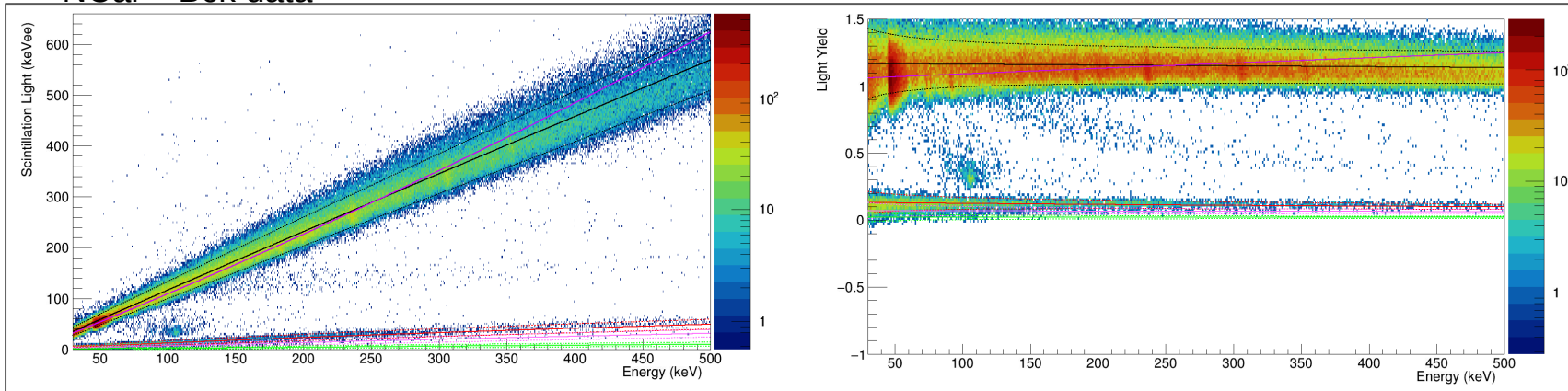


The fitted Gamma line is too low trying to “cover” the inelastic scattering of neutrons off Tungsten

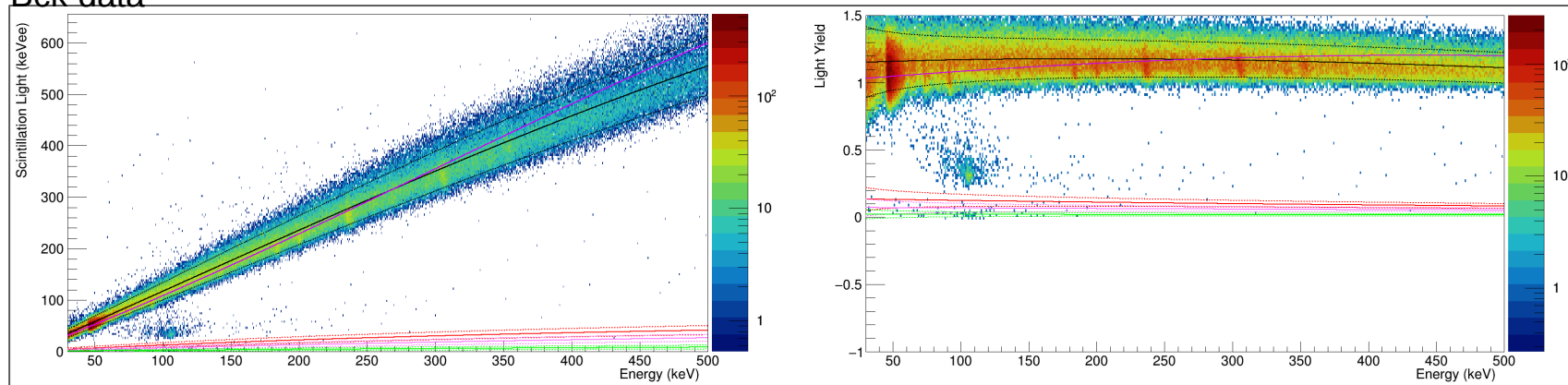


Band fit results

NCal + Bck data



Bck data



Extended Likelihood function

Likelihood \Leftrightarrow Normalized pdf

$$\mathcal{L}(\Theta | \mathbf{x}) = P(\mathbf{x} | \Theta) = \prod_{i=1}^N p(x_i | \Theta)$$

Extended Likelihood \Leftrightarrow Non-Normalized df

$$\mathcal{L}^{ext}(\Theta | \mathbf{x}) = e^{-\mathcal{N}} \prod_{i=1}^N \rho(x_i | \Theta)$$

$$\mathcal{N}(\Theta) = \int_A \rho(\mathbf{x} | \Theta) d\mathbf{x}$$

Extended Likelihood for D
detectors

$$\mathcal{L}_{tot}^{ext}(\Theta | \mathbf{x}) = e^{-\mathcal{N}_{tot}(\Theta)} \prod_{d=1}^D \left[\prod_{i=1}^N \rho_d(x_i | \Theta) \right]$$

with $\mathcal{N}_{tot}(\Theta) = \sum_{d=1}^D \left[\int_A \rho_d(\mathbf{x} | \Theta) d\mathbf{x} \right]$

Calculating the exclusion limit

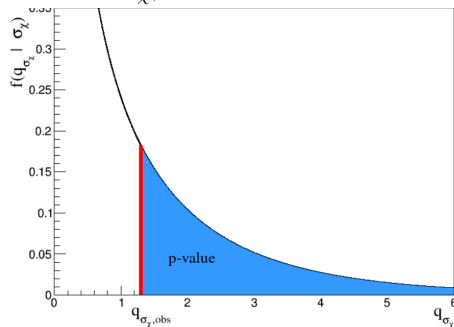
All parameters = interesting p. + nuisance p. $\longrightarrow \Theta = (\sigma_\chi, m_\chi, \delta, \theta)$

Profiled values of the parameters

Profile Likelihood test statistics $q_{\sigma_\chi} = \begin{cases} -2 \ln(\lambda(\sigma_\chi)) & \text{if } \hat{\sigma}_\chi > 0 \\ 0 & \text{if } \hat{\sigma}_\chi < 0 \end{cases}$ with $\lambda(\sigma_\chi) = \frac{\mathcal{L}(\sigma_\chi, \hat{\theta} | m_\chi, \delta, \mathbf{x})}{\mathcal{L}(\hat{\sigma}_\chi, \hat{\theta} | m_\chi, \delta, \mathbf{x})}$

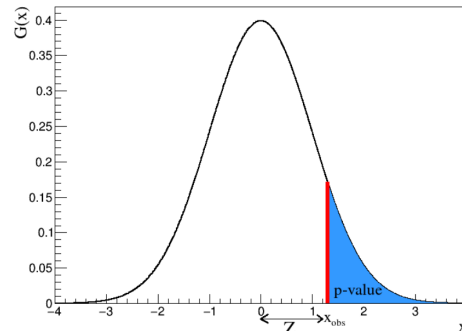
Best fit values

$$p_{\sigma_\chi} = \int_{q_{\sigma_\chi, obs}}^{\infty} f(q_{\sigma_\chi, obs} | \sigma_\chi) dq_{\sigma_\chi}$$



$$Z = \Phi^{-1}(1 - p)$$

$$Z_{\sigma_\chi} = \sqrt{q_{\sigma_\chi, obs}}$$



$$\ln(\mathcal{L}(\sigma_\chi, \hat{\theta} | m_\chi, \delta, \mathbf{x})) = \ln(\mathcal{L}(\hat{\sigma}_\chi, \hat{\theta} | m_\chi, \delta, \mathbf{x})) - \frac{Z^2}{2}$$

Migdal effect

